(2)

Carderock Division
Naval Surface Warfare Center
Bethesda, MD 20084–5000

CDNSWC–SME–CR–16–92 November 1992
Ship Materials Engineering Department
Research and Development Report

Two-Parameter Fracture Mechanics Theory and Applications

by
N.P. O'Dowd
Imperial College, London

C.F. Shih
Brown University

CDNSWC–SME–CR–16–92 Two-Parameter Fracture Mechanics Theory and Applications

ABSTRACT

A family of self-similar fields provides the two parameters required to characterize the full range of high- and low-triaxiality crack tip states. The two parameters, J and Q, have distinct roles: J sets the size scale of the process zone over which large stresses and strains develop, while Q scales the near-tip stress distribution relative to a high triaxiality reference stress state. An immediate consequence of the theory is this: it is the toughness values over a range of crack tip constraint that fully characterize the material's fracture resistance. It is shown that Q provides a common scale for interpreting cleavage fracture and ductile tearing data thus allowing both failure modes to be incorporated in a single toughness locus.

The evolution of Q, as plasticity progresses from small scale yielding to fully yielded conditions, has been quantified for several crack geometries and for a wide range of material strain hardening properties. An indicator of the robustness of the J-Q fields is introduced; Q as a field parameter and as a pointwise measure of stress level is discussed.

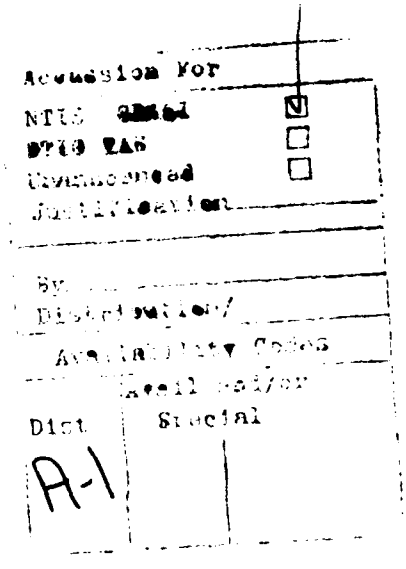

CONTENTS

LIST OF FIGURES

LIST OF TABLES

ADMINISTRATIVE INFORMATION

The work reported herein was funded under the Elastic-Plastic Fracture Mechanics of LWR Alloys Program at the Annapolis Detachment, Carderock Division, Naval Surface Warfare Center, Contract number N00167-92-K-0038. The Program is funded by the U.S. Nuclear Regulatory Commission under Interagency Agreement RES-78-104. The Technical Program monitor is Dr. S.N. Malik at the USNRC. Technical monitoring of the contract was performed by Mr. Richard E. Link (CDNSWC 2814).

1. INTRODUCTION

A two-parameter fracture theory can be motivated by considering the progression of plastic states as loading on a cracked body is increased. At low loads, the near-tip stresses and deformations evolve according to a self-similar field, scaled by Rice's J-integral [1]. This field, characterized by a high level of stress triaxiality, also describes the evolution of the near-tip stresses and deformations in certain crack geometries as plastic flow progresses from well-contained yielding to large scale yielding. While this high triaxiality field is only one of many possible states that can exist under fully yielded conditions, it is the only field that has received careful study until recently. When the high triaxiality field (Hutchinson [2], Rice and Rosengren [3], Rice and Johnson [4], McMeeking [5]) prevails over distances comparable to several crack tip openings, J alone sets the near-tip stress level and the size scale of the zone of high stresses and deformations. Considerable efforts have been directed to establishing, for different crack geometries, the remote deformation levels which ensure that the near-tip behavior is uniquely measured by J (McMeeking and Parks [6], Shih and German [7]). The end result is a framework, based on J and the high triaxiality crack tip field, for correlating crack growth over a range of plane strain yielding conditions (see review articles by Hutchinson [8], Parks [9]) and for relating critical values of the macroscopic parameter J_{IC} to fracture mechanisms operative on the microscale (see review article by Ritchie and Thompson [10]).

Arguments that a single parameter might not suffice to characterize the near-tip states of fully yielded crack geometries have been raised by McClintock [11]. He noted that non-hardening plane strain crack tip fields of fully yielded bodies are not unique but exhibit levels of stress triaxiality that depend on crack geometry. Though high stress triaxiality is maintained in geometries involving predominantly bending on the uncracked ligament, the level of crack tip stress triaxiality in geometries dominated by tension loads generally decreases as yielding progresses into the fully plastic state (see Refs 6 and 7). Indeed, experimentally measured $J-$resistance curves for center-cracked panels exhibit significantly higher slopes than those for compact specimens (Begley and Landes [12]).

Undoubtedly, there is merit to the latter point of view and it is the purpose of this paper to show that this viewpoint can be properly reconciled by a two-parameter $J-Q$ theory proposed by O'Dowd and Shih [13,14] and Shih *et al.* [15,16]. They showed, through full-field finite element calculations, that the $J-Q$ fields dominate over physically significant size scales, i.e. they represent the environment in which the ductile and brittle failure mechanisms are operative. An approach based on higher-order asymptotics has been suggested by Li and Wang [17] and pursued by Sharma and Aravas [18] and Chao *et al.* [19]. Extending the analysis in Refs 17 and 18, Xia *et al.* [20] have obtained up to

five terms in the asymptotic series and showed that the collective behavior of the series is consistent with the $J-Q$ field.

An alternative two-parameter approach based on J and the elastic $T-$stress has been advocated by Betegón and Hancock [21], Al-Ani and Hancock [22], Du and Hancock [23], Parks [24], Hancock *et al.* [25] and Wang [26,27]. Under circumstances where it is applicable, the $J-T$ theory can be shown to be equivalent to the $J-Q$ theory. This is discussed in the section on small scale yielding. The toughness scaling approach of Dodds *et al.* [29] can also be shown to be consistent with the $J-Q$ theory (see Kirk *et al.* [30]).

2. J–Q THEORY

Consider a cracked body of characteristic dimension L loaded remotely by a stress denoted by σ^{∞}. The scale of crack tip deformation is measured by J/σ_0 where σ_0 is the material's tensile yield stress. It can be shown from dimensional grounds that when $L \gg J/\sigma_0$ all near-tip fields are members of a single family of crack tip fields. Each member field is characterized by its level of deformation as measured by J/σ_0 and its level of crack tip stress triaxiality, as measured by Q, which also identifies that field as a particular member of the family. For example, the self-similar solution of Rice and Johnson [4] and McMeeking [5] or the HRR field (Refs 2 and 3) can be taken as the $Q=0$ member field. In short, the $Q-$family of fields provides the proper characterizing parameters for the full range of near-tip fracture states.

The weak coupling between deformation and stress triaxiality in a plastically deforming material provides another argument in favor of a two parameter description of near tip states. Since plastic flow is incompressible, the superposition of a purely hydrostatic stress state induces only an elastic volume change. Consider a plastically deforming material element in the forward sector of a crack as depicted in Fig. 1. We can superpose a hydrostatic stress $Q\sigma_0$ with little or no effect on the deformation state. It follows that near tip deformation and stress triaxiality cannot be scaled by a single parameter such as J. A second parameter is required to quantify the level of crack tip stress triaxiality. Clearly this argument does not apply to the back sector since traction free conditions must be satisfied on the crack faces. However this is of no physical consequence since the fracture processes occur in the forward sector, which is therefore the region of interest.

A size scale must enter into the fracture description. We focus on fields ahead of the crack that are relevant on the scale of the crack opening displacement δ_t, or J/σ_0, representing the environment in which the failure mechanisms are operative.

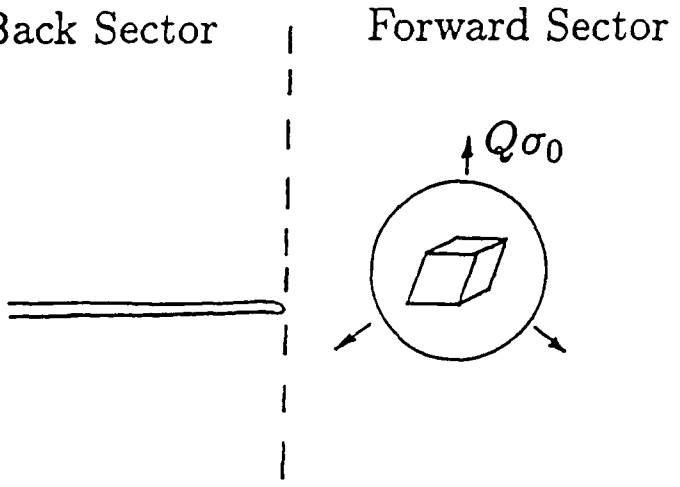

Figure 1. Schematic illustrating the necessity for a hydrostatic stress parameter and a deformation parameter to characterize the full range of near tip states in the forward sector.

2.1 Q-Family of Fields — MBL formulation

It proves convenient to construct the $Q-$family of fields using a modified boundary layer (MBL) formulation in which the remote tractions are given by the first two terms of the small-displacement-gradient linear elastic solution (Williams [31]),

$$\sigma_{ij} = \frac{K_I}{\sqrt{2\pi r}} \tilde{f}_{ij}(\theta) + T\delta_{1i}\delta_{1j}. \tag{2.1}$$

Here δ_{ij} is the Kronecker delta; r and θ are polar coordinates centered at the crack tip with $\theta = 0$ corresponding to a line ahead of the crack as shown in the insert to Fig. 2.

Fields of different crack tip stress triaxialities can be induced by applying different levels of T/σ_0. From dimensional considerations, these fields can be organized into a family of crack tip fields of the form:

$$\sigma_{ij} = \sigma_0 \overline{f}_{ij} \left(\frac{r}{J/\sigma_0}, \theta; T/\sigma_0 \right). \tag{2.2}$$

where J is Rice's $J-$integral [1]. That is, the load parameter T/σ_0 provides a convenient means to investigate and parameterize specimen geometry effects on near-tip stress triaxiality under conditions of well-contained yielding. Indeed, such studies have been carried out by Betegón and Hancock [21], Bilby *et al.* [32] and Harlin and Willis [33]. Nevertheless, the result in Equation 2.2 cannot have general applicability since the elastic

solution (Eq 2.1) upon which the $T-$stress is defined, is an asymptotic condition which is increasingly violated as plastic flow progresses beyond well-contained yielding.

Recognizing the above limitation O'Dowd and Shih [13,14], henceforth referred to as OS, identified members of the plane strain family of fields by the parameter Q which arises naturally in the plasticity analysis. OS write:

$$\sigma_{ij} = \sigma_0 f_{ij}\left(\frac{r}{J/\sigma_0}, \theta; Q\right), \quad \epsilon_{ij} = \epsilon_0 g_{ij}\left(\frac{r}{J/\sigma_0}, \theta; Q\right), \quad u_i = \frac{J}{\sigma_0} h_i\left(\frac{r}{J/\sigma_0}, \theta; Q\right). \tag{2.3}$$

The additional dependence of f_{ij}, g_{ij} and h_i on dimensionless combinations of material parameters is understood. The form in Equation 2.3 constitutes a one-parameter family of self-similar solutions, or in short a Q-family of solutions. The annular zone over which Equation 2.3 accurately quantifies the actual field is called the $J-Q$ annulus. Representative distributions of the Q family of fields are presented in Fig. 4 of Ref 1 and Fig. 1 of Ref 2.

2.2 Difference Field and Near-Tip Stress Triaxiality

Using the modified boundary layer formulation, and considering a piecewise power law hardening material, OS generated the full range of small scale yielding plane strain solutions, designated by $(\sigma_{ij})_{\text{SSY}}$. OS considered the difference field defined by

$$(\sigma_{ij})_{\text{diff}} = (\sigma_{ij})_{\text{SSY}} - (\sigma_{ij})_{\text{HRR}}, \tag{2.4}$$

where $(\sigma_{ij})_{\text{HRR}}$ is the HRR field. They systematically investigated the difference field within the forward sector, $|\theta| < \pi/2$, of the annulus $J/\sigma_0 < r < 5J/\sigma_0$, since this zone encompasses the microstructurally significant length scales for both brittle and ductile fracture (see Ref 10). Remarkably, the difference field in the forward sector displayed minimal dependence on r. Noting this behavior, OS expressed the difference field within the forward sector in the form

$$(\sigma_{ij})_{\text{diff}} = Q\sigma_0 \hat{\sigma}_{ij}(\theta), \tag{2.5}$$

where the angular functions $\hat{\sigma}_{ij}$ are normalized by requiring $\hat{\sigma}_{\theta\theta}(\theta = 0)$ to equal unity. Moreover, the angular functions within the forward sector exhibit these features: $\hat{\sigma}_{rr} \approx \hat{\sigma}_{\theta\theta} \approx$ constant and $|\hat{\sigma}_{r\theta}| \ll |\hat{\sigma}_{\theta\theta}|$ (see Figs. 3, 4 and 5 in Ref 13).

Thus the difference field within the sector, $|\theta| < \pi/2$ and $J/\sigma_0 < r < 5J/\sigma_0$, correspond effectively to a spatially uniform hydrostatic stress state of adjustable magnitude, i.e. $(\sigma_{ij})_{\text{diff}} = Q\sigma_0\delta_{ij}$. Therefore, Q defined by

$$Q \equiv \frac{\sigma_{\theta\theta} - (\sigma_{\theta\theta})_{\text{HRR}}}{\sigma_0} \qquad \text{at} \quad \theta = 0, \quad r = 2J/\sigma_0 \tag{2.6}$$

is a natural measure of near-tip stress triaxiality, or crack tip constraint, relative to a high triaxiality reference stress state. In words, Q is the difference between the actual hoop stress and the corresponding HRR stress component, the difference being normalized by σ_0. For definiteness we have evaluated Q at $r = 2J/\sigma_0$, however we point out that Q is effectively independent of distance. The distance chosen for the definition of Q lies just outside the finite strain blunting zone so that Q from a small or finite strain analysis should be nearly the same.

OS also considered the difference field whereby the standard plane strain small scale yielding solution $(\sigma_{ij})_{\mathrm{SSY;T=0}}$, which is driven by K alone, is the reference solution, i.e.

$$(\sigma_{ij})_{\mathrm{diff}} = (\sigma_{ij})_{\mathrm{SSY}} - (\sigma_{ij})_{\mathrm{SSY;T=0}}. \tag{2.7}$$

In this case the difference field in the forward sector matches a spatially uniform hydrostatic stress state even more closely. Thus an alternative definition of Q is

$$Q \equiv \frac{\sigma_{\theta\theta} - (\sigma_{\theta\theta})_{\mathrm{SSY;T=0}}}{\sigma_0} \qquad \text{at} \quad \theta = 0, \quad r = 2J/\sigma_0. \tag{2.8}$$

A definition of Q consistent with its interpretation as a triaxiality parameter is,

$$Q_m \equiv \frac{\sigma_m - (\sigma_m)_{\mathrm{SSY;T=0}}}{\sigma_0} \qquad \text{at} \quad \theta = 0, \quad r = 2J/\sigma_0, \tag{2.9}$$

where σ_m is the hydrostatic stress. We have calculated Q based on the hoop stress (Equation 2.8) and the mean stress (Equation 2.9) for the full range of T-stresses and finite width geometries. We have found that the difference between Q and Q_m is always less than 0.1. While the values of Q presented in this paper are calculated from the hoop stress via Equation 2.8 it is clear from the above that these Q values can also be used to calculate the corresponding hydrostatic stress levels.

2.3 Difference Field and Higher-Order Terms of the Asymptotic Series

The connection between the difference field and higher-order terms of the asymptotic series can be understood in the context of the MBL formulation. Here the stress field obey the functional form

$$\sigma_{ij} = \sigma_0 f_{ij}\left(\frac{r}{J/\sigma_0}, \theta; Q\right), \tag{2.10}$$

which also should apply to finite-width crack geometries as long as the characteristic crack dimension L is sufficiently large compared to J/σ_0. Now, if one assumes a product dependence on the first argument in Equation 2.10 and works within deformation plasticity theory and an elastic power-law hardening material, then one obtains a series in $r/(J/\sigma_0)$:

$$\sigma_{ij} = \sigma_0 \left(\frac{J}{\alpha\epsilon_0\sigma_0 I_n r}\right)^{1/(n+1)} \tilde{\sigma}_{ij}(\theta; n) + \underbrace{\text{second order term} + \text{higher order terms}}_{\text{Difference Field}} \tag{2.11}$$

where ϵ_0 is a reference strain, α a material constant (for a piecewise power-law material $\alpha = 1$) and I_n is an integration constant. By definition, the asymptotic series beyond the first term is equivalent to the difference field since (see previous section)

$$\sigma_{ij} = (\sigma_{ij})_{\text{HRR}} + \text{Difference Field.} \tag{2.12}$$

The HRR field and the second-order term provides only a two-term approximation to the solution for the MBL problem and this point appears not always to be understood.

The higher-order asymptotic analysis of Refs 17 and 18 has been extended by Xia, Wang and Shih [20]. They have obtained a five term expansion for the series in Equation 2.11 for $n = 3$ and four term expansions for $n = 5, 7$ and 10. Furthermore, they have successfully matched the four term series to the radial and angular variations of the difference field given in Fig. 3 and Fig. 5 in Ref 13 for an $n = 10$ material. Indeed in the forward sector $|\theta| < \pi/2$, the collective behavior of the the second, third and fourth order terms is effectively equivalent to a spatially uniform hydrostatic stress state. This observation together with the discussion of the previous section supports the simpler form for the near-tip fields:

$$\sigma_{ij} = (\sigma_{ij})_{\text{HRR}} + Q\sigma_0\delta_{ij}, \qquad |\theta| \leq \pi/2. \tag{2.13}$$

Furthermore, it may be noted that an admissible range of stress states for an elastic-perfectly plastic material can be written in the form

$$\sigma_{ij} = (\sigma_{ij})_{\text{Prandtl}} + \underbrace{Q\sigma_0\delta_{ij}}_{\text{Difference Field}}, \qquad |\theta| \leq \pi/4, \tag{2.14}$$

where $(\sigma_{ij})_{\text{Prandtl}}$ designates the Prandtl slip-line solution and again the difference field corresponds simply to a uniform hydrostatic stress state scaled by Q (see Refs 23 and 14).

2.4 Variation of Q with Distance

Because Q scales the difference field relative to a reference stress state, it provides a sensitive measure of the evolution of near-tip stress triaxiality in finite width cracked bodies. It also can be used to detect changes in the stress triaxiality that deviates from the pattern that develops under MBL loadings. For this purpose, we consider $Q(\bar{r})$ defined by

$$Q(\bar{r}) = \frac{\sigma_{\theta\theta}(\bar{r}) - [\sigma_{\theta\theta}(\bar{r})]_{\text{SSY;T=0}}}{\sigma_0}, \quad \text{at} \quad \theta = 0 \tag{2.15}$$

where $\bar{r} \equiv r/(J/\sigma_0)$. Note that $(\sigma_{\theta\theta})_{\text{SSY;T=0}}$ is chosen as the reference field.

The mean gradient of Q over $1 < \bar{r} < 5$,

$$Q' = \frac{Q(\bar{r} = 5) - Q(\bar{r} = 1)}{4} \tag{2.16}$$

can be used to monitor changes in the spatial pattern of the stress triaxiality ahead of the crack that do not conform to a spatially uniform hydrostatic stress field. In other words, Q' provides a measure of the robustness of the $J - Q$ fields for the application of interest. If $|Q'| < 0.1$ then the difference field is effectively constant over $1 < \bar{r} < 5$. If $|Q'|$ is much larger than 0.1 then the variation of the difference field over the interval $1 < \bar{r} < 5$ can be comparable to σ_0. In the latter case, Q provides only a pointwise measure of the stress level—at the distance $2J/\sigma_0$—ahead of the crack tip.

2.5 Reference Field Distributions

Table 1 provides the reference field distributions for a broad range of n values. For completeness we have included the hoop stress distributions according to the HRR singularity and the small scale yielding solutions for small strain and finite strain (piecewise-power-law hardening material; $E/\sigma_0 = 500, \nu = 0.3$). Figure 2 presents the hoop stress and mean stress reference fields established by the MBL formulation with $T = 0$. The original studies of OS were based on a finite strain formulation to ensure a full description of the near-tip states. Our subsequent studies have shown that small and finite strain analyses provide essentially identical results over the region of interest $1 < \bar{r} < 5$. This can also be seen by comparing the finite strain and small strain distributions in Fig. 2.

Two reference fields have been proposed, , $(\sigma_{\theta\theta})_{\mathrm{HRR}}$ and $(\sigma_{\theta\theta})_{\mathrm{SSY;T=0}}$. Our numerical investigations of different crack geometries show that, when the small scale yielding solution is chosen as the reference state, the difference fields correspond more closely to a uniform hydrostatic stress state over a greater range of plastic deformation. However, the choice of reference distribution used in the definition of Q remains a matter of convenience. We emphasize that once a choice is made, it must be applied consistently throughout the analysis. *We recommend that Equation 2.8 be used as the standard definition for Q with the small strain solution as the reference field. Having a standard definition facilitates the comparison of solutions obtained by different investigators and the tabulation of a handbook of Q solutions.*

While we have limited our discussion to a piecewise power-law hardening material, the $J - Q$ theory is independent of the form of the material's constitutive relation. Thus $(\sigma_{\theta\theta})_{\mathrm{SSY;T=0}}$ can be evaluated for an actual stress-strain relation. Of course, for consistency the analyses in the fracture application should also use the same stress-strain relation.

	$r/(J/\sigma_0)$	HRR	Small Strain	Finite Strain
n = 3	1	5.99	5.46	5.95
	2	5.04	4.53	4.72
	3	4.55	4.06	4.19
	4	4.24	3.76	3.85
	5	4.01	3.53	3.61
n = 5	1	4.77	4.42	4.83
	2	4.25	3.90	4.06
	3	3.97	3.63	3.73
	4	3.79	3.44	3.52
	5	3.65	3.29	3.36
n = 10	1	3.83	3.57	3.79
	2	3.59	3.35	3.52
	3	3.46	3.22	3.33
	4	3.38	3.12	3.20
	5	3.31	3.03	3.11
n = 20	1	3.37	3.21	3.06
	2	3.26	3.09	3.22
	3	3.20	3.01	3.10
	4	3.15	2.95	3.02
	5	3.12	2.89	2.96
n = ∞	1	-	2.83	2.49
	2	-	2.80	2.97
	3	-	2.77	2.91
	4	-	2.74	2.86
	5	-	2.71	2.82

Table 1. Reference stress distributions, $\sigma_{\theta\theta}/\sigma_0$, from HRR field and small and finite strain boundary layer solutions.

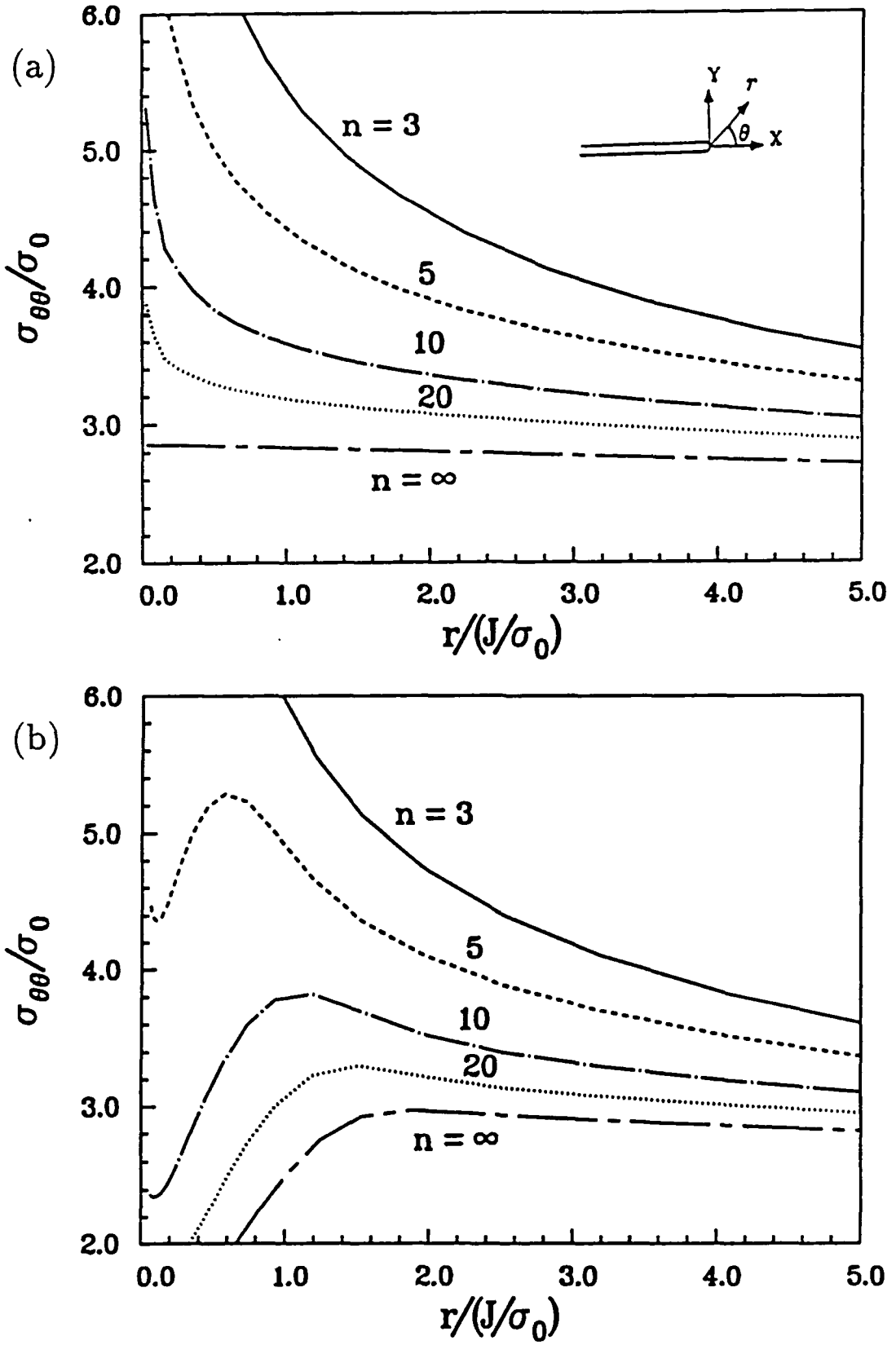

Figure 2. Plane strain reference fields for $n = 3, 5, 10, 20$ and ∞ ($E/\sigma_0 = 500, \nu = 0.3$). Hoop stress reference fields, (a) small strain (b) finite strain. Mean stress reference fields, (c) small strain (d) finite strain

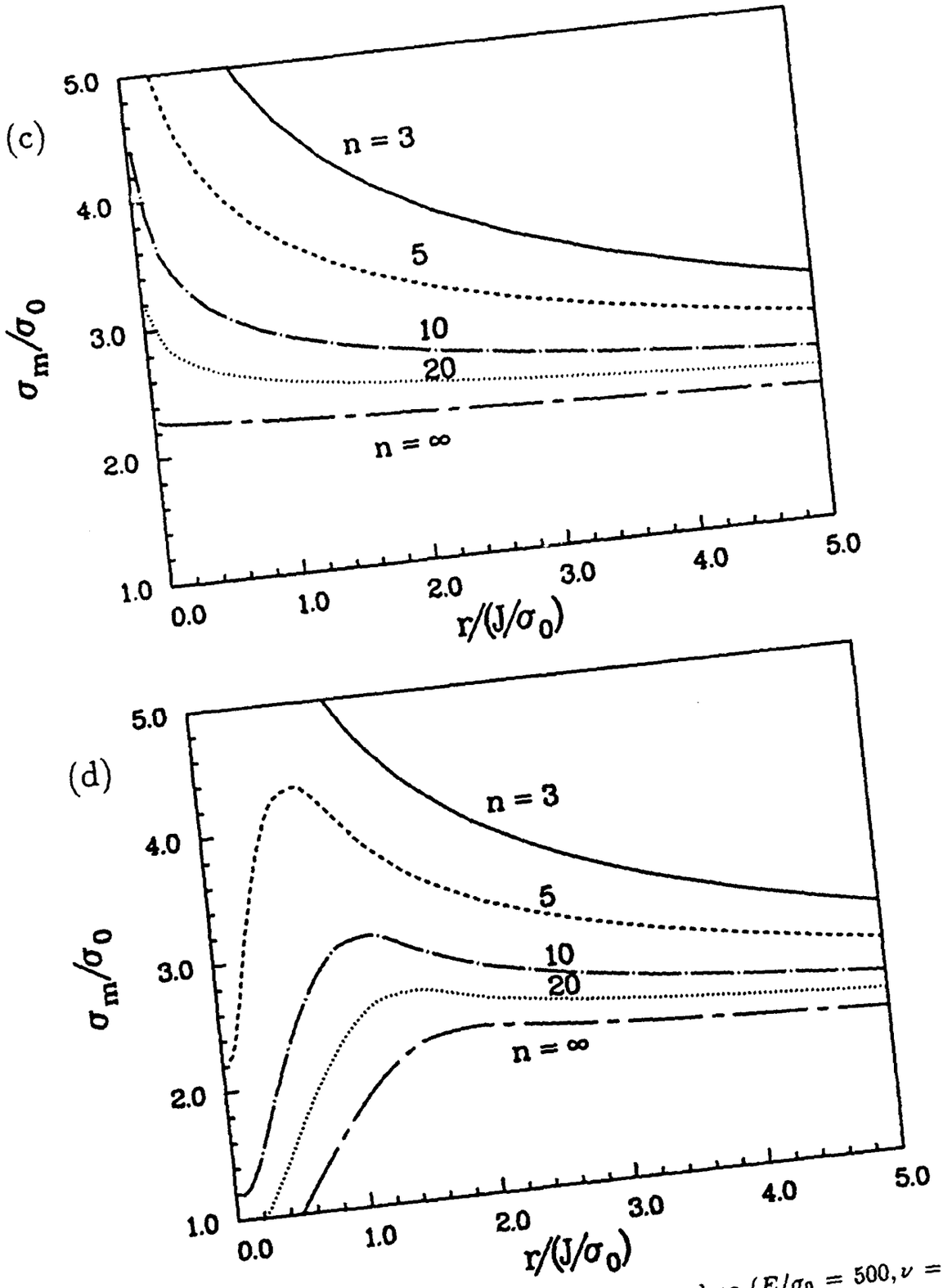

Figure 2. Plane strain reference fields for $n = 3, 5, 10, 20$ and ∞ ($E/\sigma_0 = 500, \nu = 0.3$). Hoop stress reference fields, (a) small strain (b) finite strain. Mean stress reference fields, (c) small strain (d) finite strain

2.6 Engineering Applications of the $J-Q$ Theory

For engineering applications two forms of the near tip plastic states are proposed:

$$\sigma_{ij} = (\sigma_{ij})_{\mathrm{HRR}} + Q\sigma_0\delta_{ij}, \tag{2.17}$$

and

$$\sigma_{ij} = (\sigma_{ij})_{\mathrm{SSY;T=0}} + Q\sigma_0\delta_{ij}, \tag{2.18}$$

where Q in Equations 2.17 and 2.18 are defined by Equations 2.6 and 2.8 respectively.

The values of the hoop stress of the HRR field for $1 < \tilde{r} < 5$ is given in Table 1. The other stress components can be found in Symington *et al.* [39]. The hoop and mean stress distributions of the small scale yielding field with $T = 0$ are given in Table 1 and Fig. 2. More details are found in Refs 13 and 14.

The physical interpretation of Equations 2.17 and 2.18 is this: *negative (positive) Q values mean that the hydrostatic stress ahead of the crack is reduced (increased) by $Q\sigma_0$ from the $J-$dominant stress state, or the standard small scale yielding stress state.* This interpretation is precise when $|Q'| \ll 1$.

As stated previously we recommend the use of Equation 2.18 in the $J-Q$ fracture methodology. However, the explicit representation in Equation 2.17 can facilitate analyses leading to predictions of constraint effects on toughness as outlined in the section on a cleavage toughness locus.

3. SMALL SCALE YIELDING

3.1 Q-T Relation

Within the modified boundary layer formulation, a strict one-to-one correspondence exists between Q and T (see Refs 13 and 14). For a piecewise power-law hardening material, the relationship takes the form

$$Q = F(T/\sigma_0; n), \tag{3.1}$$

with an additional weak dependence on E/σ_0 and ν, where E is Young's modulus and ν is Poisson's ratio. Curves of Q vs. T/σ_0 for $n = 3$, 5, 10, 20 and ∞ are displayed in Fig. 3. The Q values in Fig. 2 and Table 2 are based upon the definition in Equation 2.8, and were determined by small strain analyses, using $E/\sigma_0 = 500$ and $\nu = 0.3$; essentially identical results were obtained from finite strain analyses. It can be seen that Q increases monotonically with T/σ_0. Also note that crack tip stress triaxiality can be significantly lower than the reference state (the $Q = 0$ state) but cannot be elevated much above it. The values Q and Q' are given in Table 2 keeping only two places beyond the decimal point. Note that the largest value of Q' is less than 0.04. Thus Q is effectively constant over the distance $1 < \tilde{r} < 5$ for all MBL loadings.

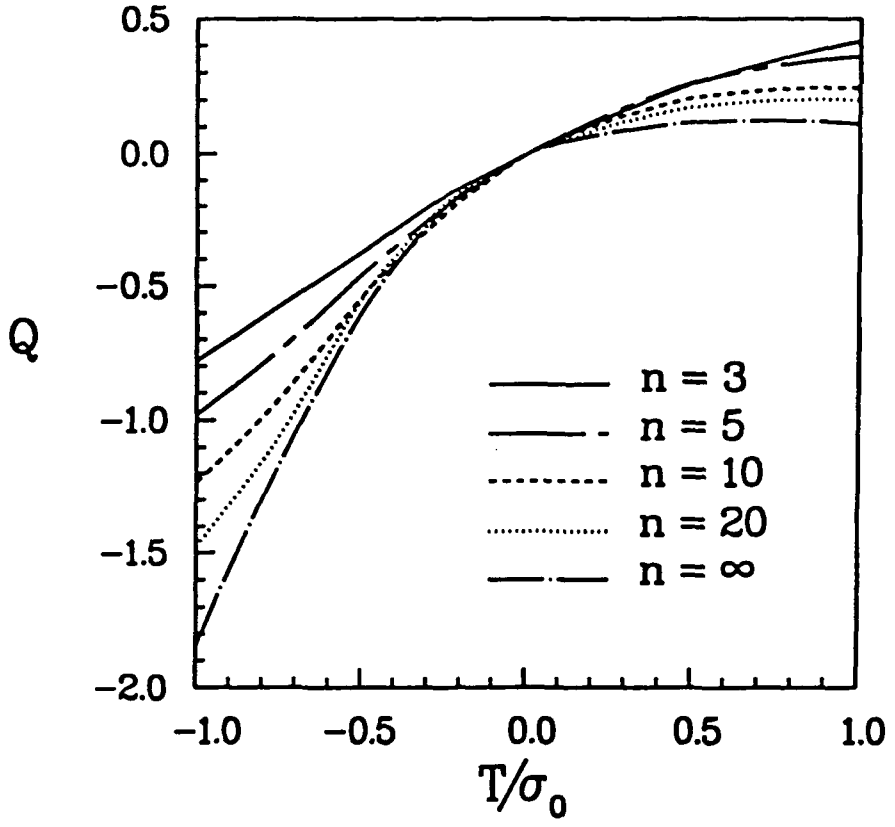

Figure 3. Variation of Q with T/σ_0 for $n = 3$, 5, 10, 20 and ∞.

T/σ_0	−1.0	−0.75	−0.5	−0.25	0.0	0.5	1.0
$n = 3$, Q	−0.78	−0.57	−0.37	−0.16	0.0	0.27	0.41
Q'	−0.02	−0.01	0.0	0.0	0.0	−0.01	−0.04
$n = 5$, Q	−0.98	−0.74	−0.46	−0.20	0.0	0.27	0.36
Q'	−0.03	0.0	0.0	0.0	0.0	0.0	−0.02
$n = 10$, Q	−1.23	−0.92	−0.54	−0.23	0.0	0.21	0.24
Q'	−0.03	0.0	0.0	0.0	0.0	0.0	0.0
$n = 20$, Q	−1.48	−1.06	−0.55	−0.19	0.0	0.17	0.20
Q'	−0.02	0.02	0.0	0.0	0.0	0.0	0.0
$n = \infty$, Q	−1.84	−1.17	−0.60	−0.21	0.0	0.12	0.12
Q'	0.03	0.03	0.0	0.0	0.0	0.0	0.0

Table 2. Values of Q and Q' for several values of T/σ_0.

n	a_1	a_2	a_3
3	0.6438	−0.1864	−0.0448
5	0.7639	−0.3219	−0.0906
10	0.7594	−0.5221	0.0
20	0.7438	−0.6673	0.1078
∞	0.6567	−0.8820	0.3275

Table 3. Polynomial coefficents for $Q-T$ relation

The curves in Fig. 3 can be closely approximated by

$$Q = a_1\left(\frac{T}{\sigma_0}\right) + a_2\left(\frac{T}{\sigma_0}\right)^2 + a_3\left(\frac{T}{\sigma_0}\right)^3. \tag{3.2}$$

The values of a_1, a_2 and a_3, obtained by least squares fitting, are listed in Table 3 for several n values. We have explored several other values of E/σ_0 and ν and found that the effect on the value of Q is negligible. The relations of Betegón and Hancock [21] and Wang [25], correlating T with near-tip hoop stress, also can be rearranged into the form of Equation 3.2.

To facilitate the use of Equation 3.2 in the analysis of finite width geometries we have provided normalized values of the the stress intensity factor K, $F(a/W)$, and the T-stress, $h_T(a/W)$ and $\Sigma(a/W)$, for a number of crack specimens in Table 4. These are taken from Sham [35,36] and Leevers and Radon [37]. The tabulated values allow us to calculate Q in these geometries under contained yielding.

3.2 $J-T$ and $J-Q$ Approaches

Two approaches to specifying families of Mode I plane strain elastic-plastic crack tip fields have been proposed. The first approach, suggested by Hancock and co-workers, utilizes the elastic $T-$stress associated with the second term of Williams' expansion (Eq 2.1) to correlate the elastic-plastic crack tip fields of varying stress triaxiality. The essence of their proposal is this — the near-tip stress triaxiality Q can be estimated by T using Equation 3.2 for loadings up to fully yielded conditions. We propose to quantify near tip constraint using the $J-Q$ theory which has a strong theoretical basis as discussed earlier.

Within the MBL formulation a description of near-tip states by J and Q is equivalent to that phrased in terms of K and T since Q and T are related by Equation 3.1 and J and K are related through

$$J = \frac{1-\nu^2}{E}K_I^2 \tag{3.3}$$

$$F(a/W)=K/\sigma^{\infty}\sqrt{\pi a}$$

a/W	CCP	DECP	TPBB
0.05	1.001	1.122	1.020
0.10	1.006	1.121	1.023
0.20	1.025	1.118	1.027
0.30	1.058	1.120	1.094
0.40	1.109	1.132	1.229
0.50	1.186	1.163	1.465
0.60	1.303	1.226	1.879
0.70	1.488	1.343	2.688
0.80	1.816	1.568	4.627
0.90	2.581	2.117	12.358

$$h_T(a/W) = T/\sigma^{\infty}$$

a/W	CCP [36]	DECP [36]	TPBB [35]
0.05	-1.001	-0.526	-0.438
0.10	-1.006	-0.526	-0.369
0.20	-1.028	-0.529	-0.239
0.30	-1.071	-0.536	-0.099
0.40	-1.142	-0.548	0.075
0.50	-1.257	-0.558	0.318
0.60	-1.450	-0.568	0.712
0.70	-1.807	-0.580	1.487
0.80	-2.559	-0.590	3.636
0.90	-4.889	-0.599	15.167

$$\Sigma(a/W) = T\sqrt{\pi a}/K$$

a/W	CCP [36]	DECP [36]	TPBB [35]
0.05	-1.000	-0.469	-0.430
0.10	-1.000	-0.469	-0.361
0.20	-1.004	-0.473	-0.233
0.30	-1.012	-0.479	-0.090
0.40	-1.029	-0.484	0.061
0.50	-1.059	-0.480	0.217
0.60	-1.113	-0.463	0.379
0.70	-1.214	-0.432	0.553
0.80	-1.409	-0.376	0.786
0.90	-1.894	-0.283	1.227

Table 4. Values of K, T and Σ for CCP, DECP and TPBB geometries.

under plane strain conditions. *However, the equivalence of the two approaches does not hold under fully yielded conditions.* The $J - Q$ fields can exist over the entire range of plastic yielding and do not depend on the existence of the elastic field (Eq 2.1). By contrast, T is undefined under fully yielded conditions. Furthermore, our numerical investigations, to be presented in the section on finite width geometries, show that the $J - T$ approach overestimates the actual stress triaxiality for some geometries and underestimates it in other cases so that there is not a consistent trend. *Stated in another way, a $T-$stress fracture methodology could be conservative for some geometries and non-conservative in others—this suggests that such an approach may be impractical.*

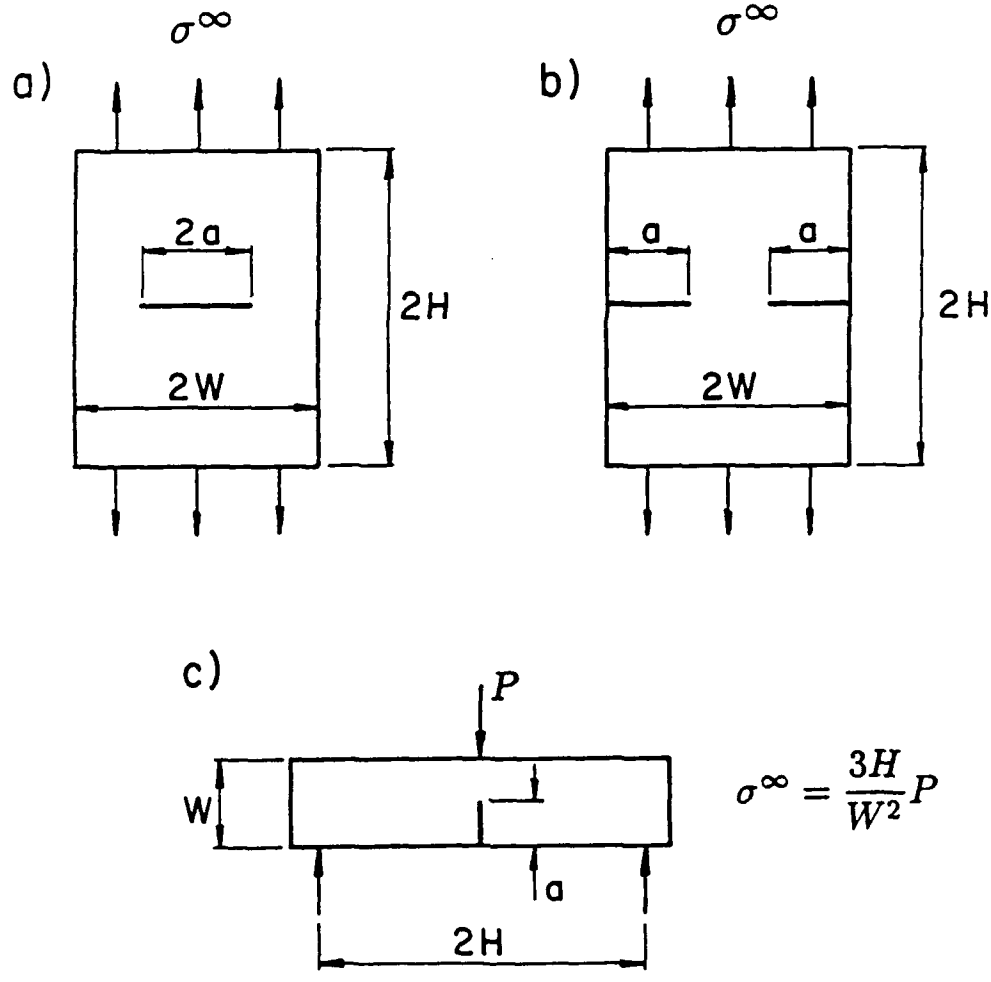

Figure 4. Fracture specimen geometries: (a) center-crack panel (b) double-edge crack panel (c) three-point-bend bar.

4. EVOLUTION OF Q IN FINITE WIDTH GEOMETRIES

$Q-$solutions have been obtained by finite element calculations for the crack geometries shown in Fig. 4. The solutions reported here were obtained by analyses based on a small strain J_2 flow theory. A typical mesh for the finite-width crack geometry has about 1000 four-node isoparametric elements. Readers are referred to Refs 13 and 14 for details on finite element meshes, plasticity formulation and solution procedure. The Q values presented in the subsequent sections are evaluated at $r/(J/\sigma_0) = 2$ unless stated otherwise. J is evaluated using the domain integral technique as discussed in Ref 38.

4.1 Center-Cracked Panel (CCP)

The evolution of Q for $n = 3$ and 5 and $n = 10$ and 20 is shown in Figs 5 and 6, respectively. Solutions are presented for the full range of crack length to width ratios: $0.05 \leq a/W \leq 0.8$. In the figures, J is normalized by the crack length a when $a/W < 0.5$ and by the remaining ligament b when $a/W \geq 0.5$. Observe that the stress triaxiality decreases steadily with increasing J and approaches a steady-state slope at fully yielded conditions.

Figure 7a and 7c show the effect of strain hardening on Q for a short crack and a deep crack, respectively. For both geometries, the loss of stress triaxiality is greater in the lower hardening materials.

The variation of Q with distance is shown in Fig. 7b and 7d. Here, Q is evaluated at $r/(J/\sigma_0) = 1$, 2, 3 , 4 and 5. It can be seen that Q has only a slight dependence on r under fully yielded conditions. For the range of loading shown in Fig. 7, $|Q'| < 0.03$ indicating that the J and Q are accurate descriptors of the field over distances $1 < r/(J/\sigma_0) < 5$.

In Fig. 7b and 7d we also provide a comparison between the actual stress triaxiality and the prediction by the T-stress via Equation 3.2 The open circles in Fig. 7b and 7d are the T stress predictions and the solid lines are the actual near-tip triaxiality. At low loads, Equation 3.2 predicts the evolution of near-tip stress triaxiality accurately. However, at fully yielded conditions, the stress triaxiality is incorrectly predicted. In the case of $a/W = 0.1$, T underestimates the stress triaxiality by about $0.5\sigma_0$. For a deep crack $a/W = 0.8$, T overestimates the stress triaxiality by a similar amount.

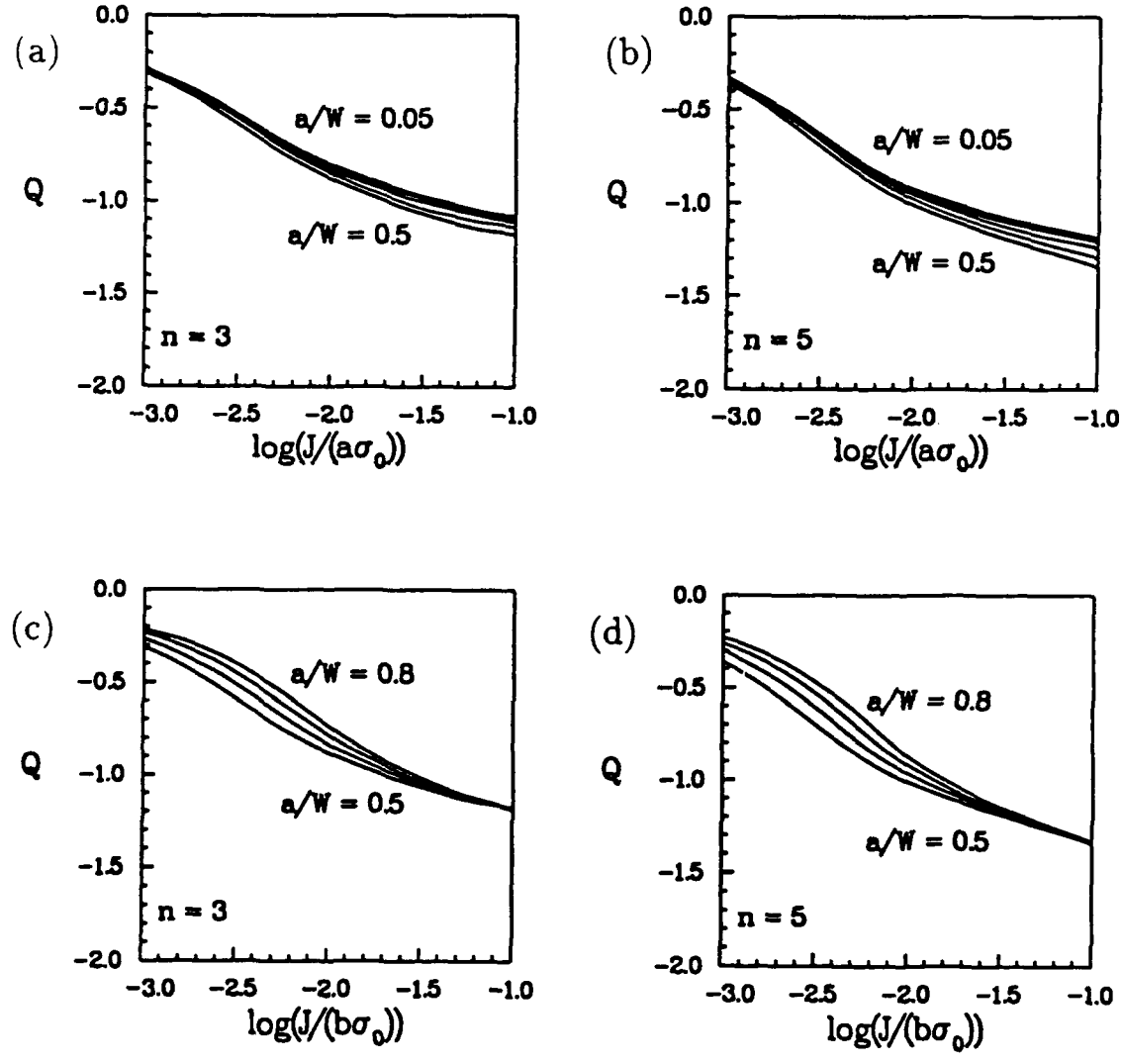

Figure 5. Center-cracked panel —evolution of Q with increasing J. $a/W = 0.05$, 0.1, 0.2, 0.3, 0.4 and 0.5, (a) $n = 3$ (b) $n = 5$; J normalized by crack length. $a/W = 0.5$, 0.6, 0.7 and 0.8, (c) $n = 3$ (d) $n = 5$; J normalized by remaining ligament.

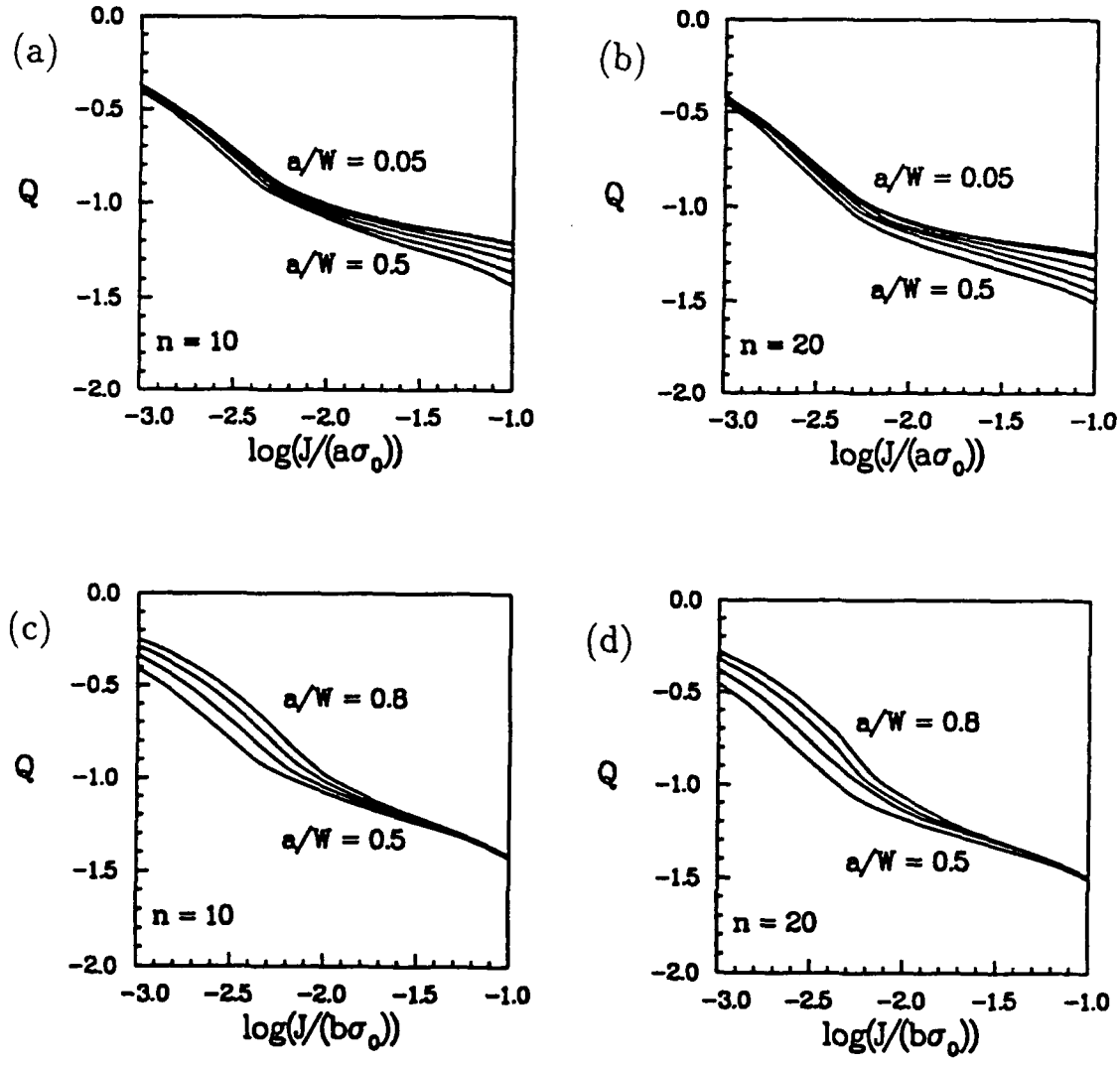

Figure 6. Center-cracked panel —evolution of Q with increasing J. $a/W = 0.05$, 0.1, 0.2, 0.3, 0.4 and 0.5, (a) $n = 10$ (b) $n = 20$; J normalized by crack length. $a/W = 0.5$, 0.6, 0.7 and 0.8, (c) $n = 3$ (d) $n = 5$; J normalized by remaining ligament.

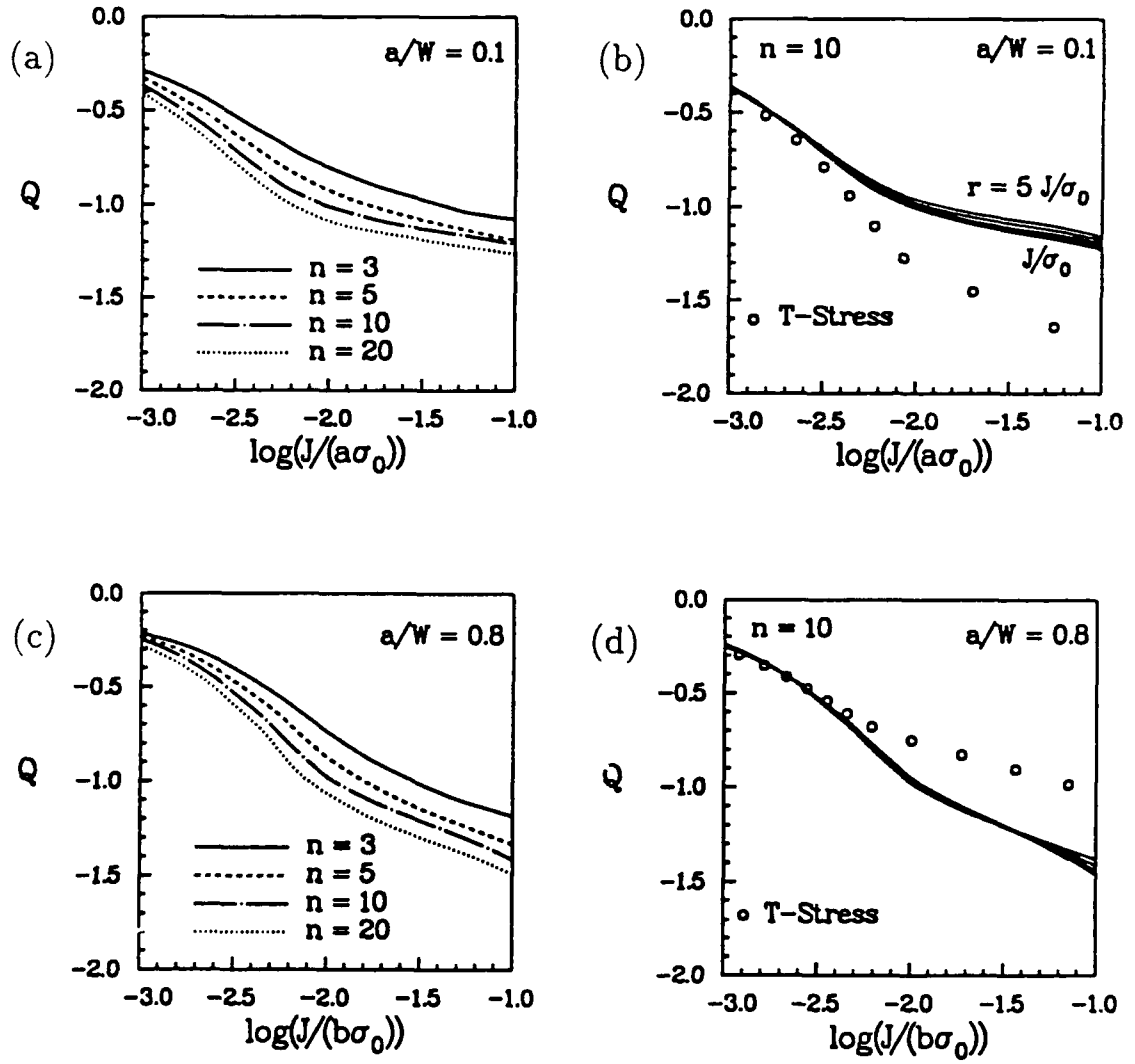

Figure 7. Center-cracked panel. Effect of n on the evolution of Q; (a) short crack, (c) deep crack. Q evaluated at $r/(J/\sigma_0) = 1$, 2, 3, 4 and 5 for $n = 10$; (b) short crack (d) deep crack. The open circles are predictions based on the $T-$stress.

4.2 Three-Point Bend Bar (TPBB)

Solutions for Q for the three-point bend bar are shown in Figs. 8 and 9 for $0.05 \leq a/W \leq 0.8$. The behavior of Q in shallow cracked specimens, $a/W < 0.3$, is similar to that seen for the center-cracked-panel, that is, the loss of stress triaxiality occurs gradually. When the crack is sufficiently deep, $a/W \geq 0.3$, high stress triaxiality is maintained for deformations characterized by $J/(a\sigma_0)$, or $J/(b\sigma_0)$, less than about 0.01. At higher J levels, the global bending stress field impinges on the near-tip region, $r \approx 2J/\sigma_0$, causing a rapid loss of stress triaxiality. This occurs at about $J/(b\sigma_0) = 0.02$ corresponding to a deformation level which is less than the ASTM limit for a valid J_{Ic} test ($J/(b\sigma_0) = 0.04$).

Strain hardening effects on the evolution of Q are displayed in Fig. 10a, 10c and 10e. It can be seen that the effect of strain hardening on Q is weak for deeply cracked bend bars, $a/W > 0.4$. The actual Q values and the $T-$stress predictions are compared in Fig. 10b, 10d and 10f. It can be seen that T correctly estimates the stress triaxiality for the short crack geometry ($a/W = 0.1$) but fails to predict the stress triaxiality under large scale yielding in the long crack geometries.

The behavior of $Q(\bar{r})$ over distances $1 \leq r/(J/\sigma_0) \leq 5$ is shown in Fig. 11 for several deformation levels as measured by $J/a\sigma_0$ or $J/b\sigma_0$. For the short crack geometry, Q is effectively independent of r over the range of loading considered. In the case of $a/W = 0.4$, Q exhibits a dependence on r when $J/a\sigma_0 \geq 0.03$ ($|Q'| \geq 0.06$); for the deepest crack geometry this behavior occurs when $J/b\sigma_0 \geq 0.017$ ($|Q'| \geq 0.07$). In both cases, the variation of Q with r is linear.

4.3 Double-Edge Cracked Panel (DECP)

Q-solutions for the double-edge cracked panel are shown in Figs. 12 and 13 for $0.1 \leq a/W \leq 0.9$. Surprisingly, high stress triaxiality under fully yielded conditions is observed only in the most deeply cracked geometry, $a/W = 0.9$. Also note that for $a/W = 0.9$ the constraint falls slighty and then rises again when the ligament is fully yielded. For shallow flaws, $a/W \leq 0.5$, Q is almost independent of relative crack size a/W.

Strain hardening effects on the evolution of Q are presented in Fig. 14a and 14c — strain hardening effects are almost non-existent for $a/W = 0.9$. The comparison between the stress triaxiality and the T-stress prediction for the double-edged cracked panel is shown in Fig. 14b and 14d. The $T-$stress approach correctly predicts the stress triaxiality for the deepest cracked geometry $a/W = 0.9$ (see Fig. 14d) but overestimates the stress triaxiality for $a/W = 0.5$ (see Fig. 14b). Figure 15 shows the behavior of $Q(\bar{r})$ over distances $1 \leq r/(J/\sigma_0) \leq 5$ for several deformation levels as measured by $J/b\sigma_0$. It can be seen that Q exhibits only slight dependence on r.

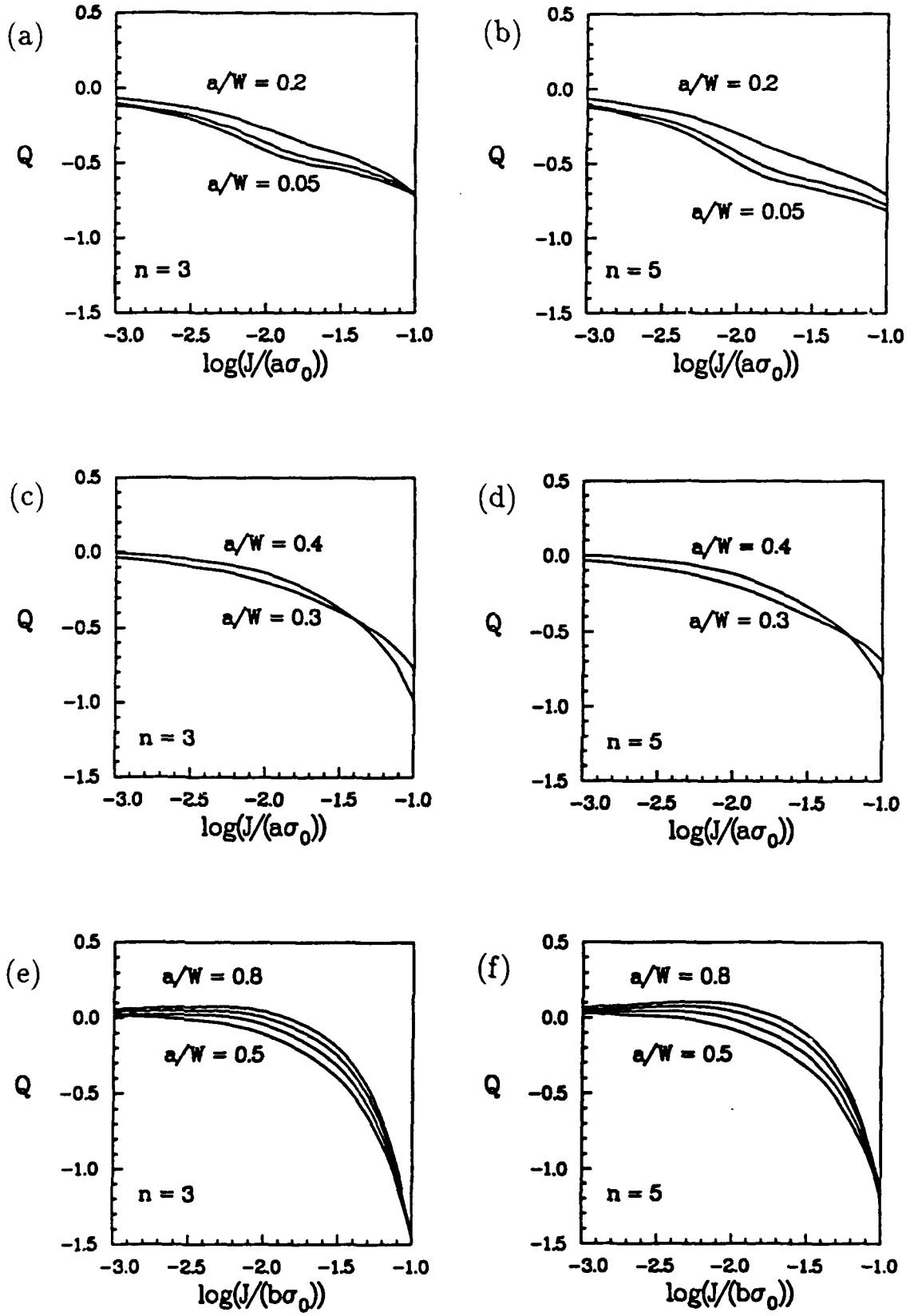

Figure 8. Three-point bend bar —evolution of Q with increasing J. $a/W = 0.05$, 0.1 and 0.2, (a) $n = 3$ (b) $n = 5$. $a/W = 0.3$ and 0.4, (c) $n = 3$, (d) $n = 5$. $a/W = 0.5$, 0.6, 0.7 and 0.8, (e) $n = 3$ (f) $n = 5$.

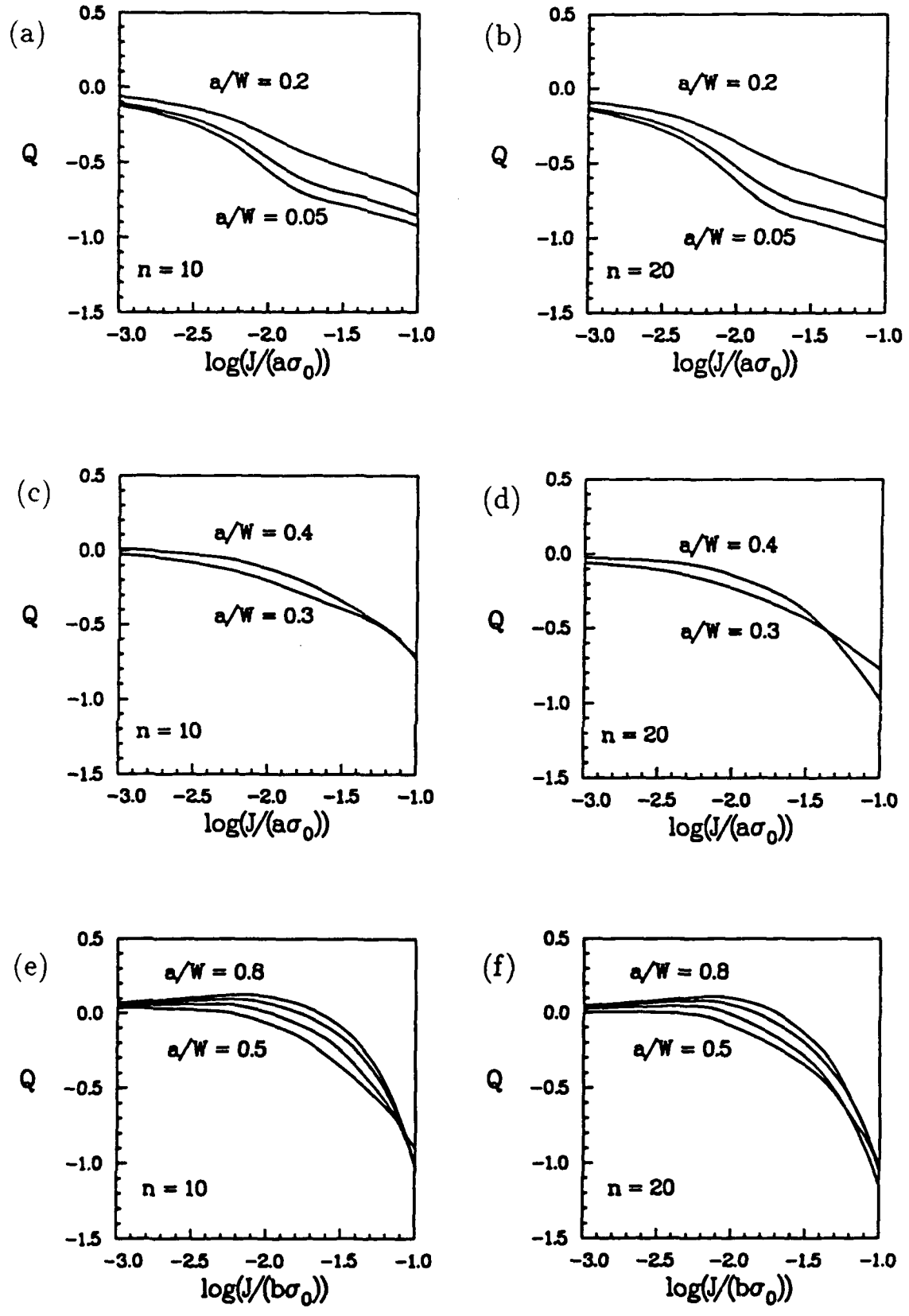

Figure 9. Three-point bend bar —evolution of Q with increasing J. $a/W = 0.05$, 0.1 and 0.2, (a) $n = 10$ (b) $n = 20$. $a/W = 0.3$ and 0.4, (c) $n = 10$ (d) $n = 20$. $a/W = 0.5$, 0.6, 0.7 and 0.8, (e) $n = 10$ (f) $n = 20$.

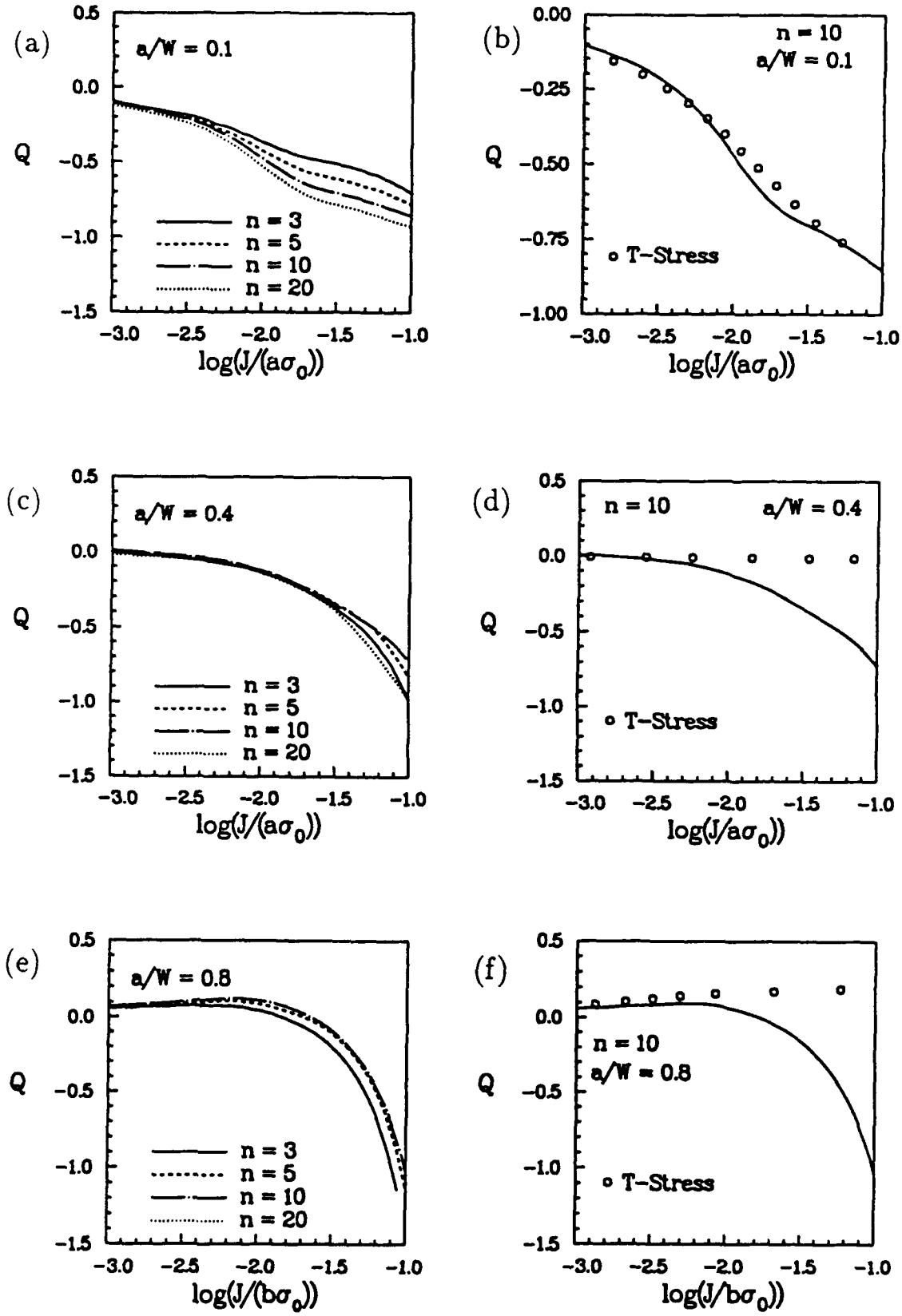

Figure 10. Three-point bend bar. Effect of n on the evolution of Q; (a) short crack, (c) intermediate crack, (e) deep crack. Comparison of Q values with predictions based on the $T-$stress; (b) short crack, (d) intermediate crack, (f) deep crack.

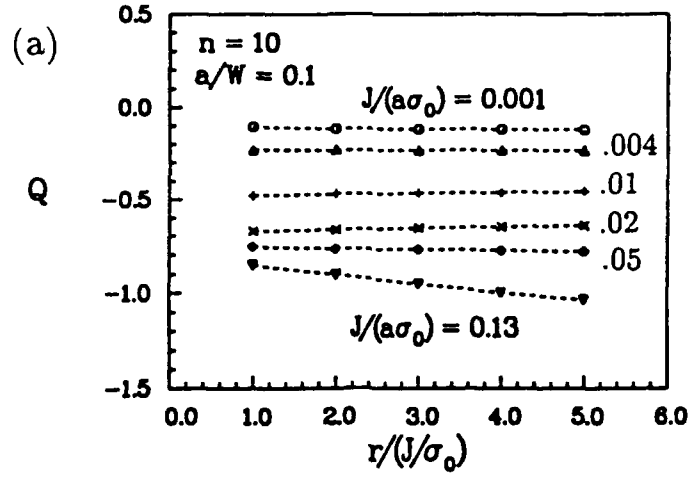

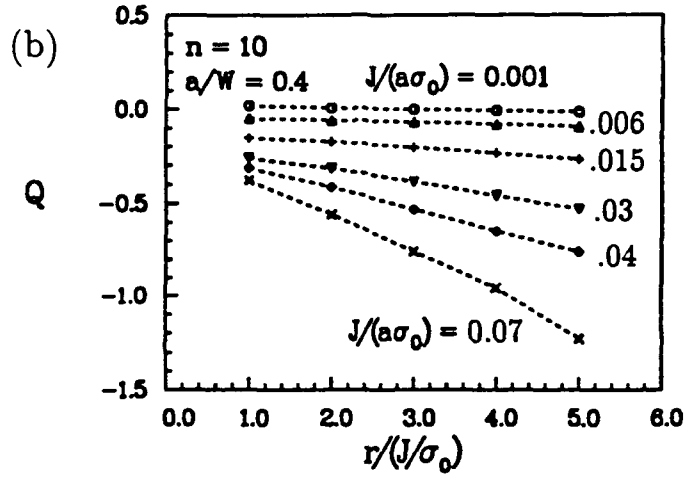

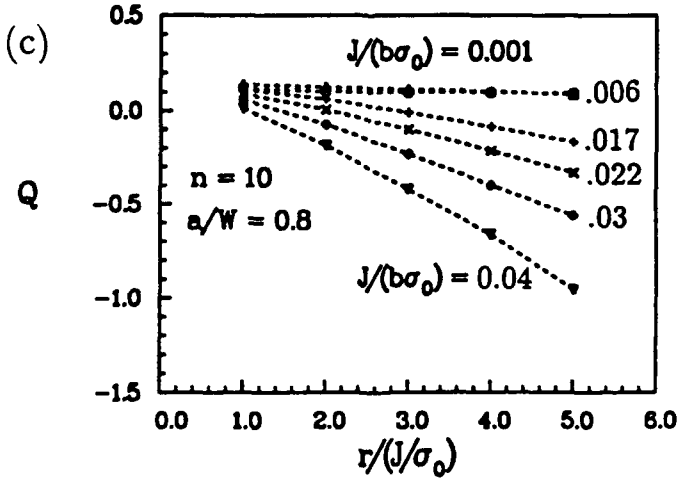

Figure 11. Three-point bend bar. Q evaluated at different positions ahead of crack tip for several deformation levels as measured by $J/L\sigma_0$. (a) short crack, $L = a$, (b) intermediate crack, $L = a$, (c) deep crack $L = b$.

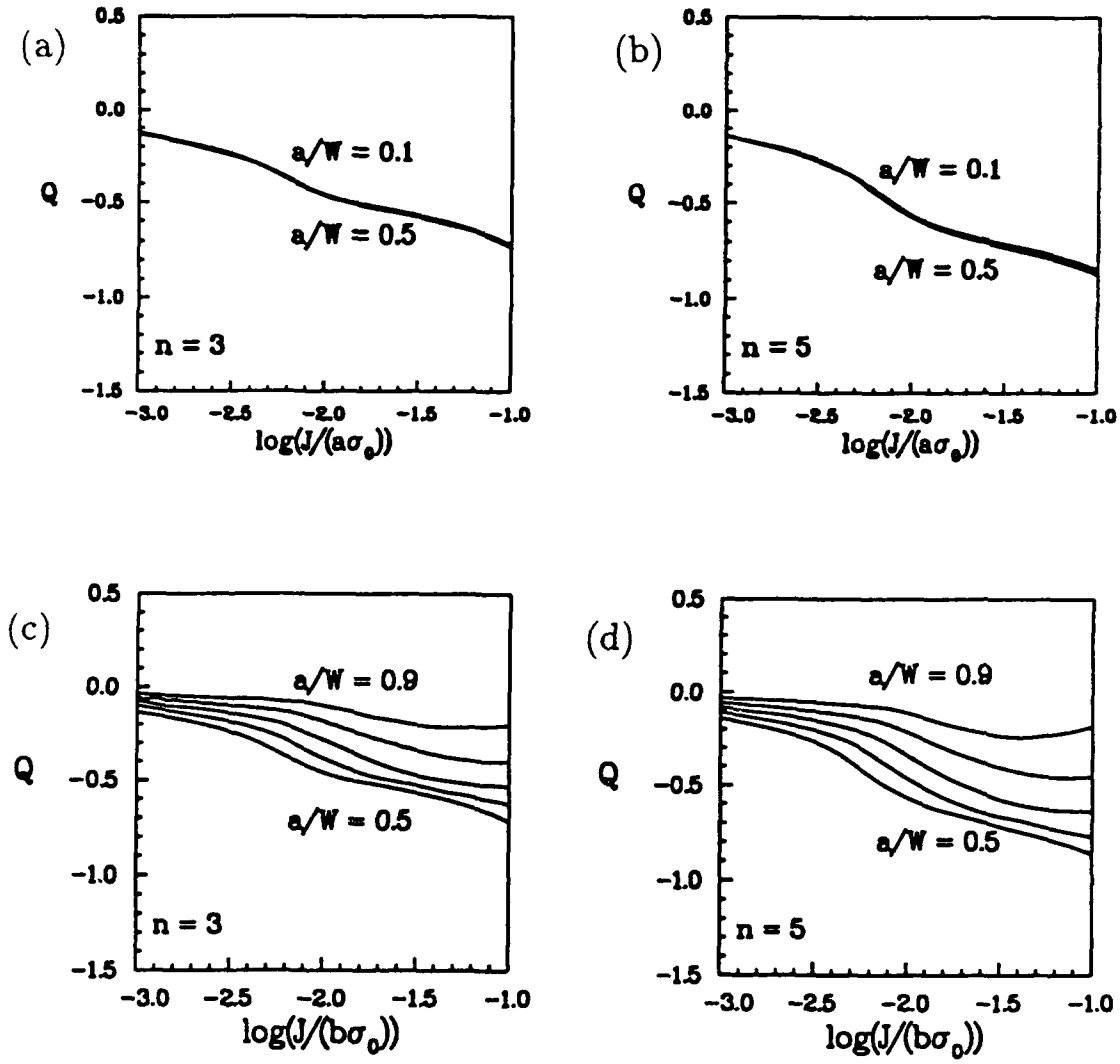

Figure 12. Double-edge cracked panel —evolution of Q with increasing J. $a/W = 0.1$, 0.2, 0.3, 0.4 and 0.5, (a) $n = 3$ (b) $n = 5$; J normalized by crack length. $a/W = 0.5$, 0.6, 0.7, 0.8, and 0.9, (c) $n = 3$ (d) $n = 5$; J normalized by remaining ligament.

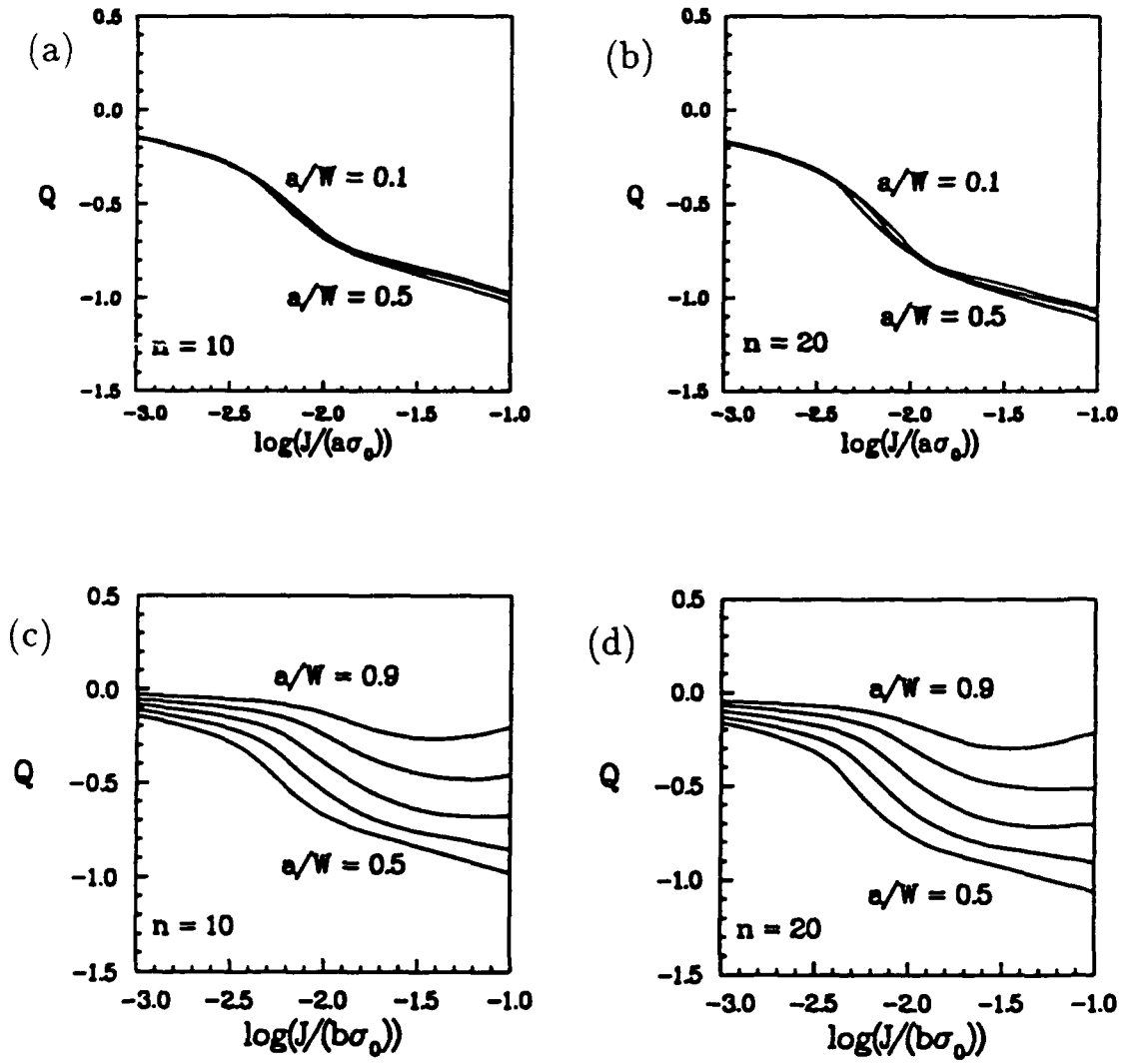

Figure 13. Double-edge cracked panel —evolution of Q with increasing J. $a/W = 0.1$, 0.2, 0.3, 0.4 and 0.5, (a) $n = 10$ (b) $n = 20$; J normalized by crack length. $a/W = 0.5$, 0.6, 0.7, 0.8, and 0.9, (c) $n = 10$ (d) $n = 20$; J normalized by remaining ligament

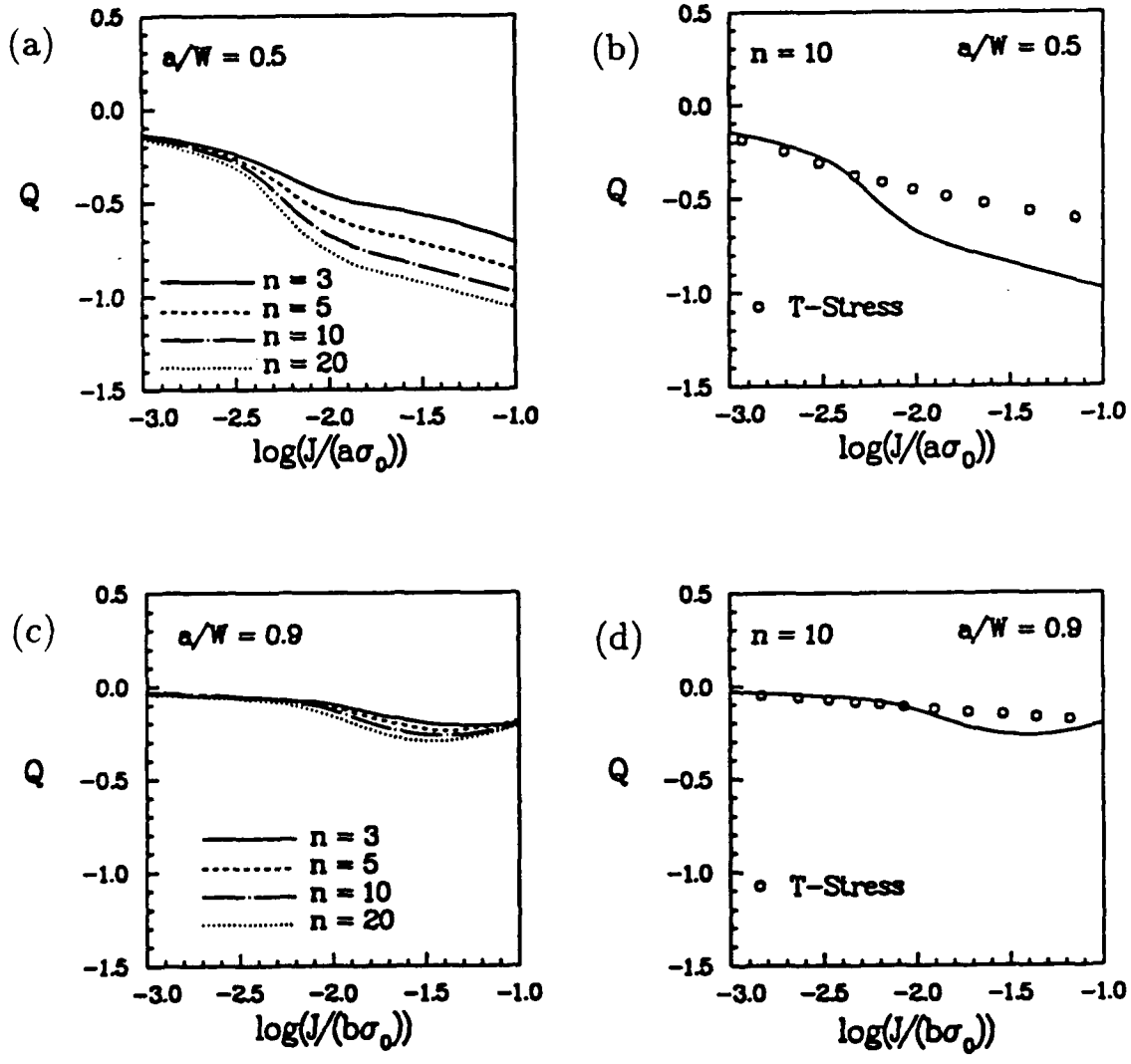

Figure 14. Double-edge cracked panel. Effect of n on the evolution of Q; (a) intermediate crack, (c) deep crack. Comparison of Q values with predictions based on the $T-$stress; (b) intermediate crack, (d) deep crack.

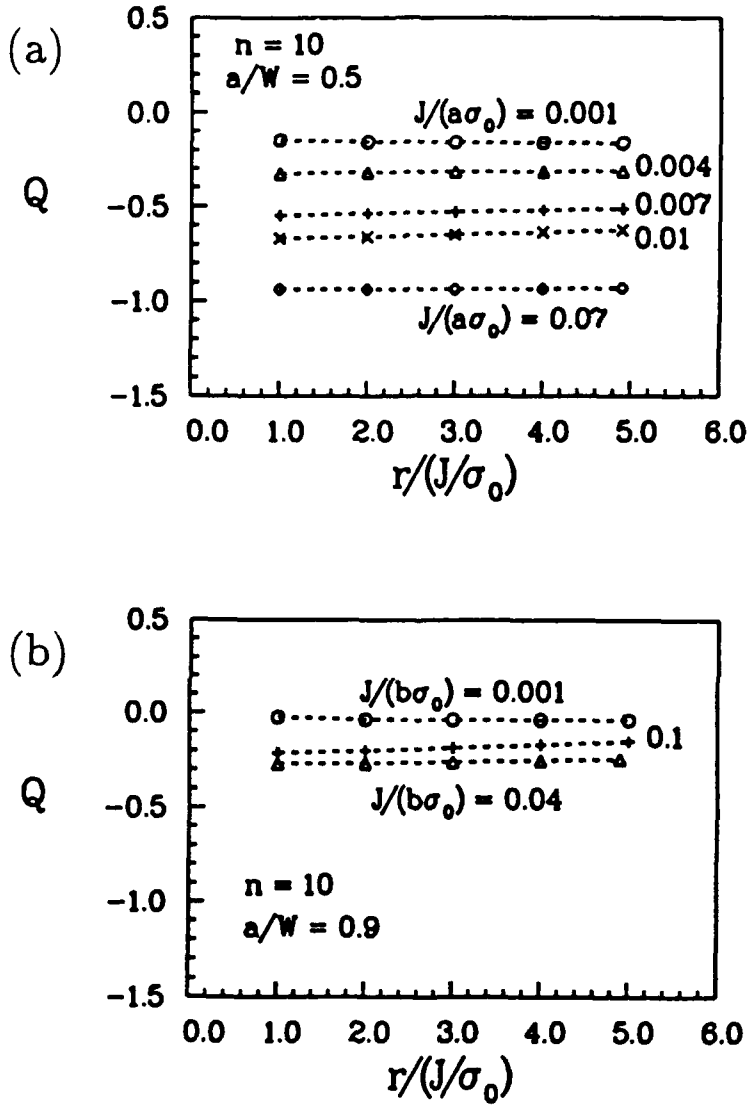

Figure 15. Double-edge cracked panel. Q evaluated at different positions ahead of crack tip for several deformation levels as measured by $J/b\sigma_0$. (a) intermediate crack, (b) deep crack.

4.4 Use of J-Q solutions

The $J - Q$ solutions provided in this and the previous section are determined from a plane strain analysis. Therefore they are applicable to crack geometries which are sufficiently thick relative to the crack size or uncracked ligament. In a typical fracture experiment J is evaluated from the load displacement record and represents a thickness-average value. The corresponding value of Q can then be obtained from the figures presented or, in the case of well-contained yielding, from Equation 3.2 in conjunction with Table 4. If the specimen conditions at fracture do not correspond closely enough to plane strain conditions, the Q solutions presented here are not strictly valid. The procedure may still be applied if we are comparing specimens of similiar thicknesses. However, if test data from specimens of widely different thicknesses are compared then 3-D solutions for Q should be used. This aspect is discussed in Refs 15 and 40 where a pointwise value of Q is used to quantify stress triaxiality near a three-dimensional crack front.

5. CLEAVAGE TOUGHNESS LOCUS

Kirk *et al.* [30] have measured cleavage fracture toughness for A515 steels at room temperature over a broad range of crack-tip constraints. They tested edge-cracked bend bars with thicknesses $B = 10$, 25.4 and 50.8 mm and various crack length to width ratios. The measured toughness data is plotted against Q in Fig. 16.

Constraint effects on fracture toughness can be predicted by using the $J - Q$ fields in conjunction with a fracture criterion based on the attainment of a critical stress, $\sigma_{22} = \sigma_c$, at a characteristic microstructural distance, $r = r_c$ (Ritchie *et al.* [34]). Within the $J - Q$ annulus the normal stress ahead of the crack is given by Equation 2.12 or more accurately by Equation 2.13. In the interest of simplicity, we work with the approximate form in Equation 2.12. Suppose that r_c is within the $J - Q$ annulus. Now impose the RKR fracture criterion to get

$$\frac{\sigma_c}{\sigma_0} = \left(\frac{J_c}{\alpha\epsilon_0\sigma_0 I_n r_c}\right)^{1/(n+1)} \tilde{\sigma}_{22}(\theta = 0) + Q. \tag{5.1}$$

Therefore, we can solve for J_c as a function of Q for selected values of σ_c and r_c. Now designate the toughness value at $Q = 0$ as J_0 and use Equation 5.1 to arrive at

$$J_c = J_0 \left(1 - \frac{Q\sigma_0}{\sigma_c}\right)^{n+1}. \tag{5.2}$$

Observe that the ratio, J_c/J_0, does not depend on r_c. The predicted variation of J_c with Q, for $\sigma_c = 3.5\sigma_0$, $J_0 = 40$ kPa·m and $n = 5$, is indicated by the dashed line in Fig.

16. It can be seen that the predicted toughness curve correctly captures the trend of the experimental data.

Sumpter and Forbes [28] have conducted extensive testing on mild steel at $-50°$ where fracure occurs by cleavage with no prior stable crack growth. Their test program includes shallow and deeply cracked bend specimens and moderate to deeply cracked center-cracked panels. Their results show that the data from fully yielded center-cracked specimens are not consistent with a $J-T$ toughness locus constructed from the bend specimens; this is not unexpected in light of our observations that the T-stress does not correctly predict crack-tip constraint under fully yielded conditions. In contrast, with allowance for experimental scatter, the data from both center-cracked and bend specimens form a single $J-Q$ toughness locus.

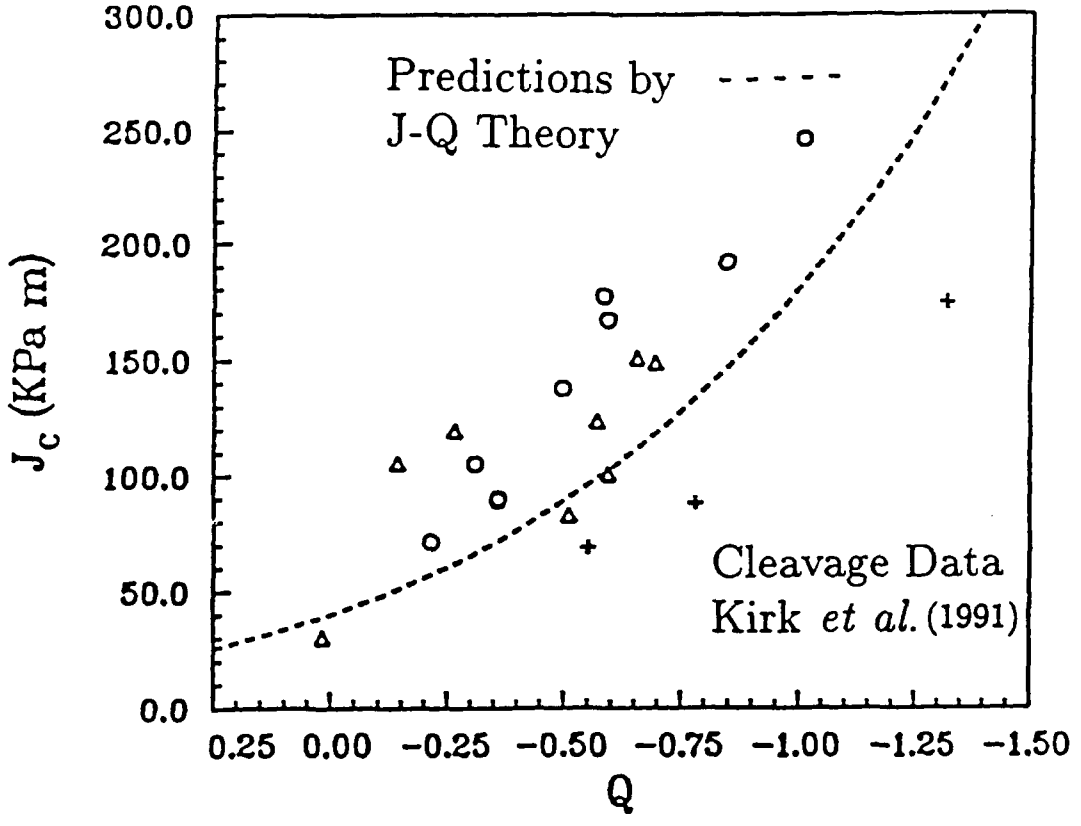

Figure 16. Cleavage toughness data for ASTM A515 Grade 70 steels tested at 20°C using edge-cracked bend bars; (Kirk *et al.*, [30]). + for thickness B=10 mm, O for B=25.4 mm, Δ for B=50.8 mm. Toughness curve predicted by $J-Q$ theory is indicated by the dashed line.

6. J-Q METHODOLOGY

The competition between fracture by cleavage and ductile tearing controls the fracture resistance of ferritic steels in the ductile-to-brittle transition region. It is well accepted that cleavage fracture is controlled by a critical hoop stress (opening stress) at a microstructurally significant distance (Refs 29, 34 and 40). There is also general agreeement that the mean stress drives cavity growth in ductile tearing (Refs 11 and 24). Since Q quantifies both the hoop *and* the mean stress relative to a reference stress state it provides a common scale to interpret brittle and ductile fracture, therefore allowing both failure modes to be incorporated in a single toughness locus.

Suppose test conditions are such that ductile and brittle mechanisms are operative. Fracture by cleavage generally occurs at high crack tip constraint while ductile tearing develops at low constraint; this is illustrated by the two distinct segments to the toughness loci shown in Fig. 17a. Since measured toughness values generally exhibit scatter, both the lower and higher toughness loci are indicated which define bounds for brittle and ductile failure. Toughness values over the full range of crack tip constraints can be measured by using the test geometries depicted in Fig. 17a. As an example, deeply cracked bend specimens generate high crack tip stress triaxiality, i.e. $Q \approx 0$. They produce driving force curves which rise steeply and therefore intersect the toughness loci within a well-defined, narrow zone of the $J - Q$ diagram. In contrast, center cracked panels and single edge crack panels loaded in tension are low constraint crack geometries. They produce driving force curves which rise with shallower slopes and thus intersect the toughness loci over a broad zone in the $J - Q$ diagram. The shallow driving force curves of low constraint crack geometry can explain the considerable scatter in cleavage values, J_c, observed in testing shallow crack specimens loaded in tension.

Utilization of the toughness locus in fracture assessments is illustrated in Fig. 17b. Suppose that the material's fracture resistance under service conditions is characterized by the indicated cleavage-ductile failure band. The driving force curve for a structure with high crack-tip constraint, structure A, rises rapidly in the $J - Q$ space so that cleavage fracture occurs when the driving force curve intersects the failure locus. In contrast, a low constraint geometry, structure B, induces a gradually rising driving force curve so that ductile tearing is the likely event at accidental overload.

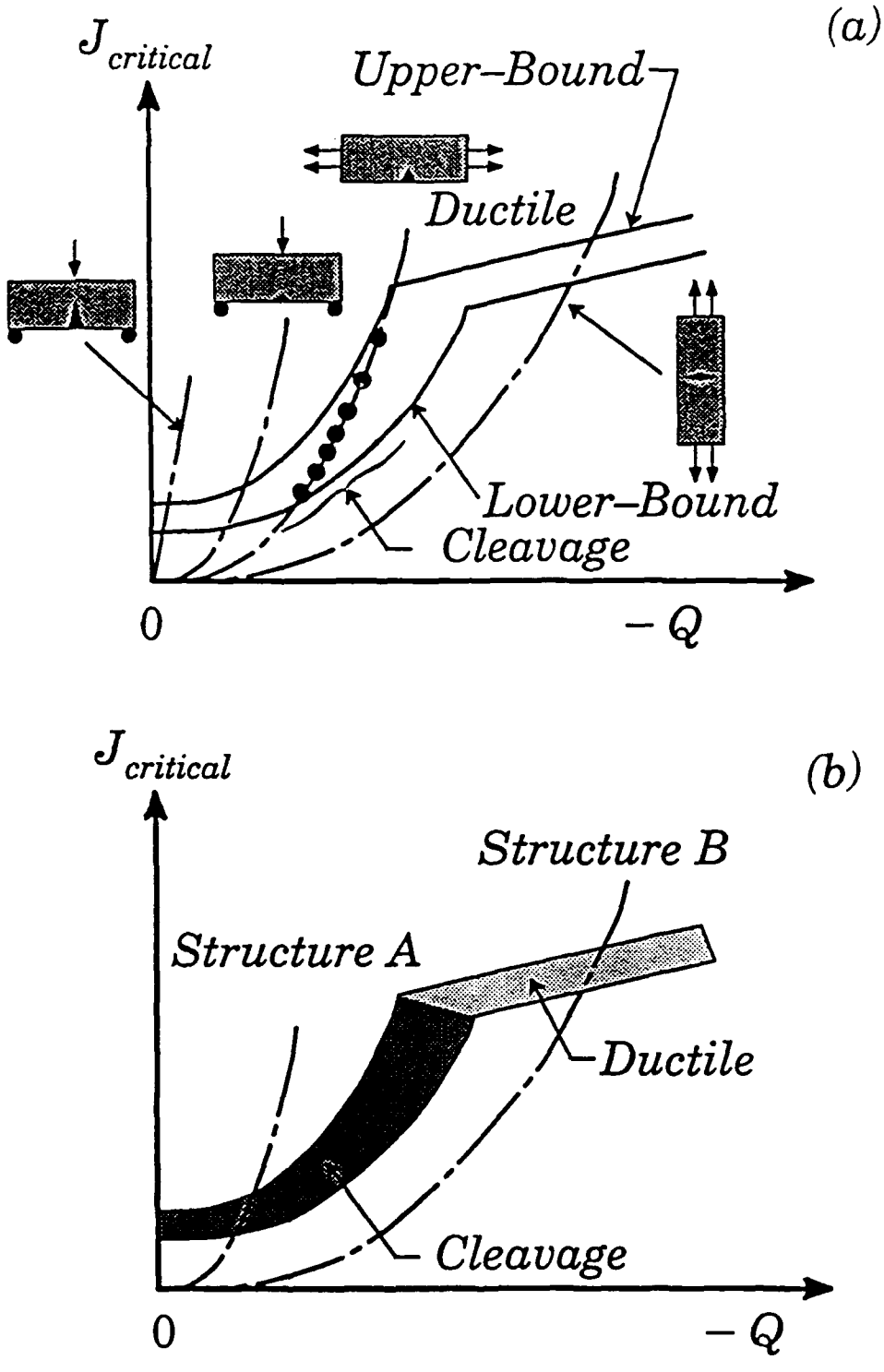

Figure 17. Illustration of $J-Q$ methodology. (a) Laboratory testing of specimens of varying constraints to measure the material's fracture resistance. Circles indicate anticipated scatter in the measured cleavage toughness data which define the upper and lower bounds. (b) Evaluation of structures using measured toughness locus and predicted $J-Q$ load path for two structural geometries.

REFERENCES

[1] Rice, J. R., "A Path Independent Integral and the Approximate Analysis of Strain Concentration by Notches and Cracks", *Journal of Applied Mechanics*, Vol. 35, 1968, pp. 379-386.

[2] Hutchinson, J. W., "Singular Behavior at the End of a Tensile Crack in a Hardening Material", *Journal of Mechanics and Physics of Solids*, Vol. 16, 1968, pp. 13-31.

[3] Rice, J. R. and Rosengren, G. F., "Plane Strain Deformation Near a Crack Tip in a Power-Law Hardening Material", *Journal of Mechanics and Physics of Solids*, Vol. 16, 1968, pp. 1-12.

[4] Rice, J. R. and Johnson, M. A., "The Role of Large Crack Tip Geometry Changes in Plane Strain Fracture", in *Inelastic Behavior of Solids*, (M.F. Kanninen et al., Eds.), McGraw-Hill, New York, 1970, pp. 641-671.

[5] McMeeking, R. M., "Finite Deformation Analysis of Crack-Tip Opening in Elastic-Plastic Materials and Implications for Fracture", *Journal of Mechanics and Physics of Solids*, Vol. 25, 1977, pp. 357-381.

[6] McMeeking, R. M. and Parks, D. M., "On Criteria for J-Dominance of Crack-Tip Fields in Large-Scale Yielding", in *Elastic-Plastic Fracture Mechanics ASTM STP 668*, American Society for Testing and Materials, Philadelphia, 1979, pp. 175-194.

[7] Shih, C. F. and German, M. D., "Requirements for a One Parameter Characterization of Crack-Tip Fields by the HRR Singularity", *International Journal of Fracture*, Vol. 17, 1981, pp. 27-43.

[8] Hutchinson, J. W., "Fundamentals of thePhenomenological Theory of Non-Linear Fracture Mechanics", *Journal of Applied Mechanics*, Vol. 50, 1983, pp. 1042-1051.

[9] Parks, D. M., "Three-Dimensional Aspects of HRR-Dominance", in *Defect Assessment in Components - Fundamentals and Applications*, ESIS/EGF9 Mechanical Engineering Publications, London, 1991, pp. 205-231.

[10] Ritchie, R. O. and Thompson, A. W., "On Macroscopic and Microscopic Analyses for Crack Initiation and Crack Growth Toughness in Ductile Alloys", *Metallurgical Transactions A*, Vol. 16A, 1985, pp. 233-248.

[11] McClintock, F. A., "Plasticity Aspects of Fracture", in *Fracture: An Advanced Treatise, Vol. III,* (H. Liebowitz, Ed.), Academic Press, New York, 1971, pp. 47-225.

[12] Begley, J. A. and Landes, J. D., "Serendipity and the J-Integral", *International Journal of Fracture*, Vol. 12, 1981, pp. 764-766.

[13] O'Dowd, N. P. and Shih, C. F., "Family of Crack-Tip Fields Characterized by a Triaxiality Parameter– I. Structure of Fields", *Journal of Mechanics and Physics of Solids*, Vol. 39, 1991, pp. 989-1015.

[14] O'Dowd, N. P. and Shih, C. F., "Family of Crack-Tip Fields Characterized by a Triaxiality Parameter– II. Fracture Applications", *Journal of Mechanics and Physics of Solids*, Vol. 40, 1992, pp. 939-963.

[15] Shih, C. F., O'Dowd, N. P. and Kirk, M. T., "A Framework for Quantifying Crack Tip Constraint." To appear in ASTM-STP, 1992.

[16] Shih, C. F., O'Dowd, N. P., "A Fracture Mechanics Approach Based on a Toughness Locus," *Proceedings of TWI/EWI/IS International Conference on Shallow Crack Fracture Mechanics Tests and Applications,* Cambridge, UK, 1992.

[17] Li, Y. C. and Wang, T. C., "High-Order Asymptotic Field of Tensile Plane Strain Nonlinear Crack Problems", *Scientia Sinica (Series A)*, Vol. 29, 1986, pp. 941-955.

[18] Sharma, S. M. and Aravas, N., "Determination of Higher-Order Terms in Asymptotic Elastoplastic Crack Tip Solutions", *Journal of Mechanics and Physics of Solids*, Vol. 39, 1991, pp. 1043-1072.

[19] Chao, Y. J., Yang, S. and Sutton, M. A., "Asymptotic Analysis of the Crack Tip Fields to Determine the Region of Dominance of the HRR Solutions." Presented at the 28th Annual Technical Meeting of the Society of Engineering Science, November, 1991.

[20] Xia, L., Wang, T. C. and Shih, C.F., "Higher-Order Analysis of Crack-Tip Fields in Elastic Power-Law Hardening Materials, " 1992. To appear in *Journal of Mechanics and Physics of Solids.*

[21] Betegón, C. and Hancock, J. W., "Two-Parameter Characterization of Elastic-Plastic Crack-Tip Fields", *Journal of Applied Mechanics*, Vol. 58, 1991, pp. 104-110.

[22] Al-Ani, A. M. and Hancock, J. W., "J-Dominance in Short Cracks in Tension and Bending", *Journal of Mechanics and Physics of Solids*, Vol. 39, 1991, pp. 23-43.

[23] Du, Z.-Z., and Hancock, J. W., "The Effect of Non-Singular Stresses on Crack-Tip Constraint", *Journal of Mechanics and Physics of Solids*, Vol. 39, 1991, pp. 555-567.

[24] Parks, D. M., "Advances in Characterization of Elastic-Plastic Crack-Tip Fields." in *Topics in Fracture and Fatigue* (edited by A. S. Argon), pp. 59-98, Springer Verlag, 1992.

[25] Hancock, J. W., Reuter, W. G. and Parks, D. M., "Constraint and Toughness Parameterized by T." To appear in ASTM-STP, 1992.

[26] Wang, Y.-Y., "On the Two-Parameter Characterization of Elastic-Plastic Crack-Front Fields in Surface-Cracked Plates." To appear in ASTM-STP, 1992.

[27] Wang, Y.-Y., "A Two-Parameter Characterization of Elastic-Plastic Crack Tip Fields and Applications to Cleavage Fracture", Ph.D. Thesis, Department of Mechanical Engineering, MIT, 1991.

[28] Sumpter, J. D. G. and Forbes, A.T., "Constraint Based Analysis of Shallow Cracks in Mild Steel", *Proceedings of TWI/EWI/IS International Conference on Shallow Crack Fracture Mechanics Test and Applications*, Cambridge, UK, 1992.

[29] Dodds, R. H., Jr., Anderson, T. L. and Kirk, M. T., "A Framework to Correlate a/W Effects on Elastic-Plastic Fracture Toughness (J_c)," *International Journal of Fracture*, Vol. 48, 1991, pp. 1-22.

[30] Kirk, M. T., Koppenhoefer, K. C., and Shih, C. F., "Effect of Constraint on Specimen Dimensions Needed to Obtain Structurally Relevant Toughness Measures." To appear in ASTM-STP, 1992.

[31] Williams, M. L., "On the Stress Distribution at the Base of a Stationary Crack", *Journal of Applied Mechanics*, Vol. 24, 1957, pp. 109-114.

[32] Bilby, B. A., Cardew, G. E., Goldthorpe, M. R. and Howard, I. C., "A Finite Element Investigation of the Effect of Specimen Geometry on the Fields of Stress and Strain at the Tips of Stationary Cracks", *Size Effects in Fracture*, 1986, Institution of Mechanical Engineers, London, pp. 37-46.

[33] Harlin, G. and Willis, J.R., "The Influence of Crack Size on the Ductle-Brittle Transition", *Proceedings of the Royal Society,* Vol. A 415, 1988, pp. 197-226.

[34] Ritchie, R.O., Knott, J.F. and Rice, J.R., "On the Relationship Between Critical Fracture Stress and Fracture Toughness in Mild Steel', *Journal of Mechanics and Physics of Solids*, Vol. 21, 1973, pp. 395-410.

[35] Sham, T. L., "The Determination of the Elastic T-Term Using Higher Order Weight Functions", *International Journal of Fracture*, Vol. 48, 1991, pp. 81-102.

[36] Sham, T. L., private communication. Manuscript in preparation.

[37] Leevers, P. S. and Radon, J. C., "Inherent Stress Biaxiality in Various Fracture Specimen Geometries", *International Journal of Fracture*, Vol. 19, 1982, pp. 311-325.

[38] Shih, C.F., Moran, B., Nakamura, T., "Energy Release Rate Along a Three-Dimensional Crack Front in a Thermally Stressed Body", *International Journal of Fracture*, Vol. 30, 1986, pp.79-102.

[39] Symington, M., Shih, C.F. and Oritz, M., "Tables of Plane Strain Mixed-Mode Plastic Crack Tip Fields" Brown University Report, MRG/DMR-8714665/1, 1988.

[40] Dodds, R.H. Jr. and Shih, C.F., "Continuum and Micro-Mechanics Treatment of Constraint in Fracture" Submitted for publication.

INITIAL DISTRIBUTION

OUTSIDE CENTER

Copies

1 DDRE/Lib

1 CNO/OP 098T

2 OCNR
- 1 1132 (Rajapakse)
- 1 1132 (Vasudivan)
- 1 0225
- 1 432S
- 1 Lib

1 NAVPGSCOL

1 USNROTCU
NAVADMINU MIT

2 NRL
- 1 Code 6380
- 1 Code 6384

8 NAVSEA
- 1 (SEA05M)
- 1 (SEA05M2)
- 1 (SEA05P)
- 1 (SEA05P1)
- 1 (SEA05P2)
- 1 (SEA05P3)
- 2 (SEA08S)

2 DTIC

5 USNRC
- 1 (M. Mayfield)
- 2 (Dr. S.N. Malik)
- 1 (A. Hiser)
- 1 (Dr. E.M. Hackett)

1 DOE, Oak Ridge

2 NIST, Boulder
- 1 Lib
- 1 (J. Berger)

4 NIST, Washington
- 1 Lib
- 1 (R. Fields)
- 1 (R. DeWitt)
- 1 (J.T. Fong)

2 Brown Univ.
- 2 (Dr. C.F. Shih)

1 Univ. of Illinois
- 1 (Dr. R.H. Dodds, Jr.)

1 Texas A&M Univ.
- 1 (Dr. T.L. Anderson)

2 NASA/Langley
- 1 Lib
- 1 (Dr. J.C. Newman)

1 Hibbit, Karlsson and Sorenson, Inc.

CENTER DISTRIBUTION

Copies

Copies	
1	0115
1	17
1	1702
1	1703
1	172
2	172.4
1	173
2	173.3
1	174.3
1	175
1	175.1
1	28
1	2801
5	281
1	2812
1	2813
12	2814
5	2814 (R. Link)
1	2815
1	3421
1	3422

NAVSSES

1	043
1	043.1
1	043C
1	045
1	045B

REPORT DOCUMENTATION PAGE

Form Approved
OMB No 0704-0188

1. AGENCY USE ONLY (Leave blank)	2. REPORT DATE	3. REPORT TYPE AND DATES COVERED
	NOV 1992	Interim

4. TITLE AND SUBTITLE
Two Parameter Fracture Mechanics Theory and Applications

5. FUNDING NUMBERS
N00167-92-K-0038
WU 1-2814-553

6. AUTHOR(S)
N.P. O'Dowd and C.F. Shih

7. PERFORMING ORGANIZATION NAME(S) AND ADDRESS(ES)
Brown University
Division of Engineering
Providence, RI 02912

8. PERFORMING ORGANIZATION REPORT NUMBER
NUREG/CR-5958

9. SPONSORING/MONITORING AGENCY NAME(S) AND ADDRESS(ES)
Carderock Div., Naval Surface Warfare Center
Annapolis Detachment,
Fatigue and Fracture Branch
Annapolis, MD 21402-5067

10. SPONSORING MONITORING AGENCY REPORT NUMBER
CDNSWC/SME
CR-16092

11. SUPPLEMENTARY NOTES
Prepared under sponsorship of the U.S. Nuclear Regulatory Commission under Interagency Agreement RES-78-104

12a. DISTRIBUTION AVAILABILITY STATEMENT
Approved for public release; distribution is unlimited

12b. DISTRIBUTION CODE

13. ABSTRACT (Maximum 200 words)

A family of self-similar fields provides the two parameters required to characterize the full range of high and low triaxiality crack tip states. The two parameters, J and Q, have distinct roles: J sets the size scale of the process zone over which large stresses and strains develop, while Q scales the near-tip stress distribution relative to a high triaxiality reference stress state. An immediate consequence of the theory is this: it is the toughness values over a range of crack tip constraint that fully characterize the material's fracture resistance. It is shown that Q provides a common scale for interpreting cleavage fracture and ductile tearing data thus allowing both failure modes to be incorporated in a single toughness locus. The evolution of Q, as plasticity progress from small scale yielding to fully yielded conditions, has been quantified for several crack geometries and for a wide range of material strain hardening properties. An indicator of the robustness of the J-Q fields is introduced; Q as a field parameter and as a pointwise measure of stress level is discussed.

14. SUBJECT TERMS	15. NUMBER OF PAGES
Constraint, stress triaxiality, elastic-plastic fracture, fracture toughness, crack initiation, cleavage, ductile tearing, J-integral & finite element method.	16. PRICE CODE

17. SECURITY CLASSIFICATION	18. SECURITY CLASSIFICATION	19. SECURITY CLASSIFICATION OF ABSTRACT	20. LIMITATION OF ABSTRACT
Unclassified	Unclassified	Unclassified	Unclassified